Positive Diagnosis of Ancient Leprosy and Tuberculosis Using Ancient DNA and Lipid Biomarkers

Helen D. Donoghue [1],*, G. Michael Taylor [2], Graham R. Stewart [2], Oona Y. -C. Lee [3], Houdini H. T. Wu [3], Gurdyal S. Besra [3] and David E. Minnikin [3]

[1] Centre for Clinical Microbiology, University College London, London, NW3 2PF, UK
[2] Department of Microbial Sciences, FHMS, University of Surrey, Guildford, GU2 7XH, UK; gm.taylor@surrey.ac.uk (G.M.T.); g.stewart@surrey.ac.uk (G.R.S.)
[3] Institute of Biology and Infection, School of Biosciences, University of Birmingham, Edgbaston, Birmingham B15 2TT, UK; o.y.lee@bham.ac.uk (O.Y.-C.L.); h.wu.2@bham.ac.uk (H.H.T.W.); g.besra@bham.ac.uk (G.S.B.); d.e.minnikin@bham.ac.uk (D.E.M.)
* Correspondence: h.donoghue@ucl.ac.uk; Tel.: +44-779-46-35271

Abstract: Diagnosis of leprosy and tuberculosis in archaeological material is most informative when based upon entire genomes. Ancient DNA (aDNA) is often degraded but amplification of specific fragments also provides reliable diagnoses. Cell wall lipid biomarkers can distinguish ancient leprosy from tuberculosis and DNA extraction residues can be utilized. The diagnostic power of combined aDNA and lipid biomarkers is illustrated by key cases of ancient leprosy and/or tuberculosis. Human tuberculosis was demonstrated in a woman and child from Atlit-Yam (~9 ka) in the Eastern Mediterranean and in the 600 BCE Egyptian "Granville" mummy. Both aDNA and lipids confirmed Pleistocene tuberculosis in a ~17 ka bison from Natural Trap Cave, Wyoming. Leprosy is exemplified by cases from Winchester (10th–12th centuries CE) and Great Chesterford (5th–6th centuries CE). A mixed infection from Kiskundorozsma, Hungary (7th century CE) allowed lipid biomarkers to assess the relative load of leprosy and tuberculosis. Essential protocols for aDNA amplification and analysis of mycolic, mycolipenic, mycocerosic acid, and phthiocerol lipid biomarkers are summarized. Diagnoses of ancient mycobacterial disease can be extended beyond the reach of whole genomics by combinations of aDNA amplification and lipid biomarkers, with sole use of the latter having the potential to recognize even older cases.

Keywords: aDNA; cell wall lipids; evolution; genotyping; *Mycobacterium leprae*; *Mycobacterium tuberculosis*; palaeopathology

1. Introduction

Leprosy and tuberculosis are significant global human infections today and were readily recognized in the past. The predominant species responsible, *Mycobacterium leprae* and *Mycobacterium tuberculosis*, are obligate human pathogens that require a living host in which to grow. Leprosy is a chronic human infection that has declined in recent years but caused approximately 213,900 new cases in 2014 [1] mainly in South East Asia, Africa and South America. It is a major cause of preventable disability and of social exclusion due to stigma. *M. leprae* is extremely slow growing and needs to be in an intracellular environment within a host, primarily human. Tuberculosis is an expanding global disease with an estimated 10.4 million new cases reported in 2015 [2]. A high level of latent tuberculosis infections suggests co-evolution of *M. tuberculosis* and its human host [3], at least throughout the Holocene period.

Bacterial infections can be recognized in archaeological remains, initially by palaeopathology and more recently by microbial ancient DNA (aDNA) [4–6]. *M. leprae* targets Schwann cells, damaging the nerves, and in late infections further damage is caused by the host immune response. In lepromatous leprosy there is a strong humeral response that is ineffective, associated with high numbers of *M. leprae* bacilli. The resulting palaeopathology is typified by gross changes to the rhino-maxillary area including pitting or perforation in the palate and resorption of the anterior nasal spine [7]. There are inflammatory changes to the ends of the long bones plus the bones in the hands and feet due to chronic infection from skin ulcers.

Tuberculosis is spread via infectious aerosols from the lungs of an infected person. If the bacilli enter the blood stream or lymphatic system they can spread to all parts of the body. In rare cases this results in skeletal tuberculosis that can be recognized by characteristic palaeopathology. It is estimated that skeletal tuberculosis occurs in only 3–6% of tuberculosis infections [8], so the extent of tuberculosis in historical and archaeological remains was consistently under-estimated in the past. About 50% of these skeletal lesions involve the spine—chiefly in the thoracic and lumbar vertebrae—followed by the cervical area and can affect one or several vertebrae. The lesions consist of circumferential lytic areas of destruction in vertebral bodies, with minimal new bone formation. The neural arches are rarely affected. Spinal collapse and angular kyphosis (Pott's disease) is common [8]. Tuberculosis may also affect other weight-bearing joints of the body such as hip or knee and can be difficult to distinguish from other disease aetiologies. Tuberculous dactylitis (*spina ventosa*) can affect the hands, particularly of younger children under six years of age. Ribs may become infected by extension from spinal lesions, by haematogenous spread from a soft tissue focus or from direct transfer from adjacent lung tissue [8]. Extension from the spine tends to cause destructive lesions at the head or neck of the rib; haematogenous spread tends to result in lytic lesions with little reactive bone formation. Diffuse periostitis or local abscess on the visceral aspects of the rib may indicate a chronic underlying pulmonary infection, of which tuberculosis is one possibility.

A further development has been the use of organic chemical techniques to detect and identify specific mycobacterial cell wall lipids in ancient cases of tuberculosis [9,10] and leprosy [11–13]. Indeed, these specific cell wall lipids are more stable than aDNA and have confirmed suspected cases of ancient leprosy in the absence of *M. leprae* aDNA [14]. Modern genetic studies show that different genotypes of these pathogens are found in different human populations, indicating that each species has emerged from an evolutionary bottleneck with subsequent clonal expansion [3,15–18]. In both these species, genotypes can be distinguished by synonymous single nucleotide polymorphisms (SNPs) [17–19]. Strains can also be identified using variable number short tandem repeats (VNTR) [20], spoligotyping [21] and microsatellite analysis [14], although these are often unstable due to poor DNA repair and are thus unsuited to study deep phylogeny of the microorganism. Unique deletions and subsets can also be exploited to identify the main lineages and branches of the *M. tuberculosis* (MTB) complex that consists of all human and animal strains [15].

The growth of this field of paleomicrobiology is summarized in Table 1 for ancient tuberculosis [4,5,9,10,22–33] and in Table 2 for ancient leprosy [6,11,14,18,34–40], highlighting the changes in methodology over time. Detailed information for a range of studies on ancient tuberculosis is provided in Table S1 [4,5,9,10,22–33,36,41–67]. Similarly, studies on ancient leprosy are tabulated in Table S2 [6,11–14,18,20,34–40,53,68–76].

This review aims to introduce the techniques currently available for the identification of ancient tuberculosis and leprosy, summarize present knowledge and discuss the validity of particular published studies.

Table 1. Summary of methods used in *M. tuberculosis* aDNA and lipid biomarker diagnoses (See Table S1 for detailed breakdown).

Year	Techniques Introduced	Significance and Examples
1993–1994	aDNA fragment amplification: IS*6110* 123 bp and nested PCR	Proof of concept Positive results from skeletal & tissue samples [4,5]
1995–1996	aDNA fragment amplification: IS*6110* PCR Confirmed by *Sal1* digestion	MTB aDNA found in Pre-Columbian America [22] MTB aDNA found in bones without lesions [23]
1998–1999	Hot-start PCR IS*6110*, *mtp40*, *oxyR*, spoligotyping, DNA sequencing Mycolic acid biomarkers	*M. tuberculosis* specifically identified [44] MTB cell wall mycolic acids used to confirm aDNA findings [9,10]—significant as these are detected directly with no amplification
2001–2003	Additional PCR markers used including IS*1081*, outer & internal primers for TbD1 deletion region and spoligotyping	*M. africanum* found in Middle Kingdom ancient Egypt [24] MTB genotyped in 18th cent. Hungarian natural mummies [25]
2004	PCR for canine aDNA and MTB IS*6110*	A 16th century Iroquoian dog had human MTB [26]
2007–2008	PCR for IS*6110*, IS*1081*, TbD1, RD regions, *oxyR*^{285} and *pncA*^{169} Improved mycolic acid detection	First finding of *Mycobacterium bovis* in human skeletal remains [27] 'Modern MTB' in early Neolithic [28]
2012	Mycolipenic and mycocerosic acid lipid biomarkers	Specific mycolipenate and clear mycocerosate pattern confirms MTB in ~17 ka bison [29]
2012–2016	Hybridization capture with Next Generation Sequencing (NGS) Metagenomics of 18th cent. MTB Whole Genome Sequencing (WGS)	Identification of 19th cent. MTB genome [30] Mixed MTB genomes in 18th cent. Hungarians [31–33]

Table 2. Summary of methods used in *M. leprae* aDNA and lipid biomarker diagnoses (see Table S2 for detailed breakdown).

Year	Techniques introduced	Significance and examples
1994	aDNA fragment amplification, with PCR primers for large target regions (459 and 530 bp)	Proof of concept Positive results indicate excellent *M. leprae* aDNA preservation [6]
2000–2001	aDNA amplification based on specific RLEP region Nested & hemi-nested PCR used to target shorter sequences	*M. leprae* found in 11th–12th cent. Orkney, Scotland, UK [34] *M. leprae* identified in Medieval Poland, 10th and 15th century Hungary [35]
2005	Primers devised for nested PCR for both *M. leprae* aDNA and MTB IS*6110*	Leprosy/TB co-infections identified in the absence of palaeopathology [36]
2006	Used hemi-nested & VNTR typing based on repetitive sequences	Different strains of *M. leprae* identified [37]
2009	Genotyping based on SNPs Mycolic acid lipid biomarkers	SNP typing reveals human origins of *M. leprae* and migrations [18] *M. leprae* mycolic acids detected [11]
2012–2017	SNP sub-genotyping and WGS Mycocerosic acid lipid biomarkers identified	SNP sub-genotyping elucidates geographical differences between *M. leprae* from different regions [14,38–40]

2. Methods

2.1. Extraction of Microbial aDNA

Numerous studies now confirm the possibility of extracting and amplifying microbial aDNA from pathogens that may persist within human bones and other tissues (e.g., [6,41]). Microbial DNA disseminated via the bloodstream may become trapped in the mineralized tissue of the skeleton, such as hydroxyapatite, or in protected sites, such as the dental root canal and pulp chamber, where it can

remain somewhat protected from breakdown. Authentic aDNA will eventually become degraded over time, due to chemical processes such as hydrolytic depurination and oxidation that result in small DNA fragments with variable degrees of damage. Mycobacterial aDNA is generally more resistant to degradation compared to mammalian host aDNA, due to the protective presence of the bacterial cell wall and the higher proportion of guanidine and cytosine in the DNA [77]. In DNA extraction from human skeletal remains, bacterial aDNA may be co-purified with humic and fulmic acids that arise from degradation of dead organic matter in soils. These are naturally occurring inhibitors of the polymerase chain reaction (PCR) used to amplify aDNA. In addition, the breakdown products of body fluids in human or animal remains, such as blood and bile, can inhibit PCR. Therefore, the extraction procedure must deliver not only effective recovery of DNA fragments from a complex mixture of tissue debris, but also ensure lysis of any remnant mycobacteria and removal of PCR inhibitors. Perusal of the literature reveals the variety of approaches that have been used. However, the basic method includes demineralization, DNA capture or precipitation, dehydration and elution or rehydration just before DNA amplification.

For DNA extraction of archaeological skeletal or mummified material, an initial incubation step in 1xTris/EDTA buffer containing proteinase K solution can be performed at 55 °C to free cross-linkages. Incubation can be for an hour or so, up to two to three days, with regular mixing and bead beating. Once disrupted, a guanidium-based chaeotropic buffer, 6 M guanidium thiocyanate (GUSCN), is used for lysis. The reagent N-phenacylthiozolium bromide (PTB) can be used to cleave any covalent cross-links, thus enabling DNA strand separation and amplification [78]. However, PTB inhibits amplification of highly fragmented aDNA that is directly precipitated so it can be helpful to split the sample and treat one aliquot with 40 µL of 0.1 mol PTB followed by silica capture, with direct precipitation of aDNA in the second aliquot without PTB. This process copes with a range of specimen types. Moreover, it is capable of inactivating any viable mycobacteria [50], which can be an advantage in some circumstances.

Silica-based DNA extraction methods [79] have been widely evaluated and found to be most efficient. Bouwman and Brown [80] looked at several variations of this approach for aDNA applications, finding silica columns to be more efficient than slurries. However, slurries provide greater freedom for incorporating additional wash steps or scaling up for larger sample volumes. If using a commercial kit that employs columns, it must be noted that many such methods fail to efficiently recover smaller fragments (<150 bp) of DNA although these may be typical of the pathogen aDNA found in archaeological material.

When detection of mycobacterial aDNA is supported by lipid biomarker analysis, the latter can be recovered from samples that have already undergone DNA extraction if required [13,38]. This is ideal for minimizing destructive sampling or for retrospective analysis.

2.2. PCR Amplification

The amplification of aDNA requires some adjustment to the composition of the mix and the selection of targets. Because of the possibility of residual inhibitors in DNA extracts, it is helpful to include bovine serum albumin (BSA) in the mix to reduce PCR inhibition [81] and to ensure the optimal level of $MgCl_2$ for the particular samples being amplified. A concentration of 2 mM is usually satisfactory, but 3 mM may be needed when reporting PCR product with hydrolysis probes. In early work on aDNA, the importance of the target size for amplification was not realized. Neither was the difference in stability of mycobacterial aDNA compared with that of mammalian aDNA appreciated. The lipid-rich mycobacterial cell wall enabled larger DNA target regions to be used successfully in early studies. Indeed, the first report of *M. leprae* aDNA used the 36-kDa-antigen gene with 530 bp as the target sequence size [6]. A later recommendation for PCR of aDNA material was that amplicon size should be kept below 200 bp [82]. Over the years, experience has since shown that many positive cases would have been missed when the amplicon targeted was greater than 150 bp. Generally, 'the smaller the better' is the rule for aDNA work. There are practical lower limits for amplicon size, as specificity and ease of authentication are important considerations. Initially, conventional PCR was used and the

amplicons identified by agarose gel electrophoresis. Restriction enzyme digestion and cloning were also used in early studies, followed by sequencing of PCR products. Subsequently, Real Time PCR was used with fluorescent probes, which allows far shorter target sequences to be used. Amplicons in the range 90–120 bp remain practical as they still allow conventional sequencing to confirm identity and also sequencing of SNPs without the need for cloning.

Repetitive elements in genomes make good targets for aDNA PCR as the chances of detecting the pathogen template increases accordingly. Examples are the RLEP, REPLEP and LEPREP elements of *M. leprae* and IS*6110* and IS*1081* elements of *M. tuberculosis* complex mycobacteria. Another good target locus for detecting and simultaneously typing mycobacteria is the direct repeat (DR) locus, a clustered regularly interspaced, short palindromic repeat (CRISPR/*cas9*) unit in the MTB complex, with its multiple copies of inverted repeats. Any of these can be combined with a labeled hybridization probe for reporting product with specificity and convenience. An example is shown in Figure 1, generated from a medieval period case of lepromatous leprosy from Winchester skeleton 45 (Sk45). This shows the RLEP product amplified from the hand (blue trace) and a tibia (red trace) [G.M. Taylor, unpublished observation].
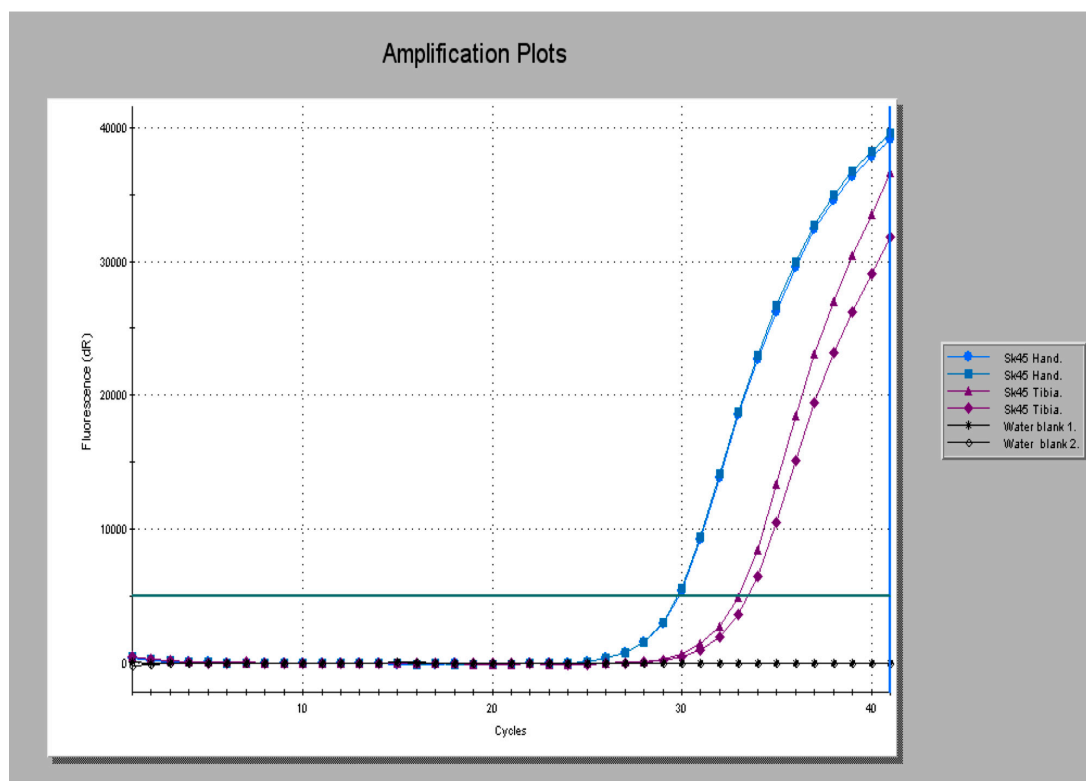

Figure 1. Real Time polymerase chain reaction (PCR) amplification profiles for a medieval period case of lepromatous leprosy (Sk45) obtained using the RLEP PCR method with product reported with a specific probe. Extracts were tested in duplicate. Product is seen amplified from the hand (blue traces) and tibia (red traces). Black traces represent non-template controls (water blanks).

In an early attempt to obtain genotyping information from ancient cases of tuberculosis, three bone samples from two separate burials, both with evidence of typical skeletal lesions, were examined [44]. These inhumations came from the cemetery site of the abbey of St. Mary Graces, on the old Royal Mint site in London, UK and were dated broadly between 1350–1538 CE, the time the cemetery was in use. One of the loci examined was for the *rpoB* gene [83] using a commercially available Inno-Lipa Rif TB kit from Innogenetics in Belgium. This kit, used in clinical diagnostics of tuberculosis, proved very useful for confirmation of the disease in these remains. The test strips have an oligonucleotide

primer specific for templates from the MTB complex, which quickly identifies/eliminates those cases where the amplicon product originates from environmental organisms other than MTB complex. The paper also describes the first use of spoligotyping [21], to examine the DR locus, and the presence of the *mtp40* gene–although this is now known not to be conclusive proof of species as it may be lost in some strains of *M. tuberculosis* as part of a deletion event analogous to RD5 of *M. bovis*. Also, amplification and Sanger sequencing of the *oxyR* pseudogene was undertaken to determine species. Finally, PCR based on an *M. bovis* specific fragment, now known to be targeting the RvD1-Rv2031c region, was performed. In both individuals, disease was shown to be due to *M. tuberculosis* rather than *M. bovis*. The spoligotypes obtained appeared to be identical and were again indicative of the human pathogen. The very same methods were later applied to nine cases of tuberculosis from a rural setting, the deserted medieval village of Wharram Percy, Yorkshire, UK [84]. At the outset of the study it was envisaged that this would very likely provide evidence of *M. bovis* infection in humans, given the close proximity of medieval farmers to their cattle. However, in six of the cases that provided genotyping data, *M. tuberculosis* was found to be responsible for the observed lesions.

The occurrence of deletions in a pathogen genome can be exploited to design extremely specific PCR methods with primers flanking the deletion and reporter fluorophores or a probe hybridizing over the deletion breakpoint. We have used this approach to distinguish between modern and ancestral strains of tuberculosis, by looking for the occurrence of deletion TbD1 [28,50] and the demonstration of bovine strains in nomadic pastoralists who had contacted this disease from their herd animals [27]. In the two examples of *M. tuberculosis* above, of an Iron Age male individual from Dorset, UK with suspected Pott's disease and a woman and infant from the 9000-year-old Neolithic site of Atlit Yam in the Eastern Mediterranean, the strains of *M. tuberculosis* had clearly already lost the TbD1 region. Therefore, so-called 'modern' TB strains are already of some antiquity. The Atlit Yam cases were also subjected to mycobacterial lipid biomarker analysis (see Section 3.2).

In the example of Iron Age nomadic pastoralists from Tuva, Southern Siberia [27], the primers used flanked the RD4 deletion, an event that has come to define classic *M. bovis* disease found in modern herd breakdowns. Another deletion PCR method applied in this study was for RD17, which showed that this event had *not* occurred, indicating the causative strains could have been due to *M. bovis* a-c lineages, but not *M. bovis* lineage d [85]. Two of these five cases infected with *M. bovis* were found in individuals radiocarbon dated to between the 4th to 2nd centuries BCE and the remaining three to between the 2nd to 4th centuries CE. The first two individuals therefore stem from the transition period between the Uyuk and Shurmak Cultures and the latter three to the Shurmak or Synnchyurek Cultures.

The study of deletions in strains from dated remains can provide limits *termini ante quem*—dates before which the deletion of interest, e.g., TbD1, had occurred. Slowly, this work is beginning to provide a timeline to anchor evolutionary models of the MTB complex. The use of deletion-based PCR overcomes the problems mentioned above in relation to specificity of the *mtp40* and the '*M. bovis* specific' fragments, which are now both known to lie *within* possible deletion regions (RD5 and RvD1-Rv2031c, respectively), so that some strains of *M. tuberculosis* and *M. bovis* will have lost these targets, confounding the outcomes.

Ancient DNA studies have also benefited from advances in hardware and the availability of core commercial kits for convenience, uniformity and the options for hot-start PCR. A kit employing a hot start *Taq* polymerase is preferred for specificity when amplifying targets from a complex *milieu*, which will invariably contain environmental bacteria. There is rarely any need for second rounds of amplification if the initial PCR method is fully optimized. Kits with non-acetylated BSA are extremely useful for counteracting PCR inhibitors or it can be added to in-house reaction mixes (1 µg/mL) without reducing reaction efficiency. The typical small aDNA PCR products may be analyzed on 3% or 4% gel electrophoresis gels with appropriate size markers. However, Real Time platforms have almost eliminated this requirement, as dissociation curve analysis and monitoring of products with labeled hybridization probes are valuable for immediate assessment of specificity. Electrophoresis gels remain useful for checking new methods and purifying amplicons for sequencing.

2.3. Diversity at Multiple Locus Variable Nucleotide Tandem Repeats (VNTRs)

A number of other loci within the genomes of both *M. leprae* and the MTB complex species exhibit variability. One important class consists of the short tandem repeat units—minisatellites and microsatellites—found in *M. leprae* [86,87]. Equivalent sites are known within *M. tuberculosis* and other complex members and have been used in standardized mycobacterial interspersed repetitive units (MIRU) VNTR typing protocols [88] and exact tandem repeats (ETR A–D) for *M. bovis* [89]. Variation at these loci arises as a result of errors in replication, such as slip-strand mispairing [90]. Such polymorphic loci have limited use for deep phylogeny as they change relatively rapidly, but we have found them valuable for differentiating between strains with the same main genotype. For example, we routinely use three such loci, one minisatellite and two microsatellite regions to distinguish between strains of *M. leprae* [20,38]. In more than a decade of typing *M. leprae* strains, we have only ever encountered the same pattern once and these were from isolates of *M. leprae* from the medieval *leprosarium* at Winchester, UK (Sks 8 and 14, see Table 3). Radiocarbon dating showed these individuals were near contemporaneous and the genetic analysis, following WGS, confirmed that the isolates were very closely related [74].

Table 3. Variable number short tandem repeats (VNTR) Sub-genotyping of *M. leprae* aDNA.

Burial	Region	Century CE	(AGA) 20	(GTA) 9	21-3	Type
Sk2	Winchester, UK	10th–12th	11	8	2	3I
Sk7	"	"	13	8	2	3I
Sk8	"	"	14	8	2	2F
Sk14	"	"	14	8	2	2F
Sk19	"	"	14	7	Fail	3I
Sk27	"	11th	12	7	2	2F
G708	Yorkshire, UK	10th–12th	10	8	3	3
GC96	Essex, UK	5th–6th	14	6	2	3I
1914	Ipswich, UK	13th–15th	12	9	2	3I
Uzbek	Uzbekistan	1st–4th	22	9	2	3L
KD271	Hungary	7th	16	24	2	3K
503	Hungary	10th–11th	18	8	2	3K
222	Hungary	10th–11th	12	12	2	3K
KK02	Turkey	8th–9th	12	11	2	3K
188	Czech Republic	9th	11	7	2	3M

2.4. Validation and the Use of Real Time Platforms

A number of criteria have arisen over the years for checking the authenticity of aDNA findings. These are summarized in Table 4. For a full consideration of authentication criteria see Taylor 2014 [91]. Real Time PCR platforms have a number of advantages for routine testing of aDNA extracts and a number of areas of synergism overlap with validation options. These, and the benefits of Real Time instruments, are included in Table 4.

Table 4. Validation of aDNA data.

Criteria	Option 1	Option 2	Option 3
Reproducibility	Run in-batch replicates	Run repeat assays	Run repeat extracts
Independent replication	Different operators (in-house)	Second centre replication	-
PCR specificity	Check T_m of melt curve and size on gel	Amplicon reported by specific probes	Amplicon sequencing
Cloning of amplicons	Cloning & sequencing to assess damage or miscoding changes	-	-
Appropriate molecular behaviour	Degraded templates Assess upper size limit	aDNA tends to high Cq values on real time platforms	Genotyping data should make phylogenetic sense

Table 4. *Cont.*

Criteria	Option 1	Option 2	Option 3
Controls	Extraction blanks to test reagents	PCR template blanks (water)	Burials lacking lesions & soil samples
Genotyping	SNP/deletion typing	VNTR analysis	NGS with controls to judge environmental contribution
Quantitative PCR	Assess aDNA at sites both with and without lesions	-	-
Independent biomarkers of disease	Mycobacterial lipid biomarkers	Recovery of peptides/proteins/sugars	-
Analysis of associated remains	Animal remains for evidence of pathogen diseases	Animal remains for evidence of faunal DNA	-

2.5. Benefits of Real Time Platforms

2.5.1. Optimization

Real Time platforms provide rapid and visible feedback for the PCR optimization matrix components (e.g., magnesium ion concentration, annealing temperature, and primer concentration). For a 100% efficient PCR reaction, there should be around 3.3 cycles difference between 10-fold template concentrations. The presence of primer-dimer will be shown by melt analysis, performed at the end of the run and can be tuned out if required by acquiring data at a higher temperature during the run.

2.5.2. Reproducibility

Product formation from replicates can be monitored easily and cheaply in real time with intercalating dyes such as EVA®Green. These are easily added to any PCR method and are inexpensive to use. The specificity of products can be checked with dissociation curves (melt temperature analysis) at the end of the run and can be tuned out if required by acquiring data at a higher temperature during the run.

2.5.3. Control Amplifications

Multiple water blanks can be included in the reaction and monitored in real time to check for any evidence of random cross-contamination. Melt analysis will reveal the lower melting temperature (T_m) of any primer-dimer compared to the target PCR amplicon. Alternatively, a probe can be used or the machine software can be set to acquire data above the T_m of non-specific products, so that these smaller molecules do not contribute to the real time amplification profile. As with conventional PCR, primer-dimer formation is a useful indicator that inhibition was not a significant factor in a negative result. There is seldom any need to include a positive control in an optimized aDNA PCR.

2.5.4. Assessing Inhibition

To rule out false negative results due to PCR inhibition, an internal control (IC) assay can be multiplexed with the locus of interest. In the competitive IC model using an artificial template, this contains the same primer annealing regions as the PCR target but with a different intermediate sequence. Amplification of this construct is monitored with a second probe designed to the central region and tagged with a different fluorophore. Alternatively, 'spiking' of unrelated PCRs with a constant amount of extracted template can help identify inhibition due to an increase in the quantification cycle (C_q) in affected samples, compared to the control C_q determined from spiking with water only. The C_q is defined as the cycle number at which fluorescence first increases above a defined threshold level.

2.5.5. Validation

Genuine aDNA positives tend to have higher C_q values and product is typically seen after more than 30 cycles of amplification, although strong positives are sometimes found. The screening PCRs we

use for *M. leprae* and MTB complex mycobacteria have been well characterized over the years and the products have been sequenced on a number of occasions. Increasingly we use specific hybridization probes that report only the amplicon of interest. Use of a short product (60–90 bp) can effectively corroborate product identity. Multiple polymorphic loci, amplified in the course of projects, are *always* sequenced to determine genotype.

3. Mycobacterial Lipid Biomarkers

3.1. Extraction of Mycobacterial Cell Wall Lipids

Mycobacteria, including *M. tuberculosis* and *M. leprae* have hydrophobic lipid-rich cell envelopes that express unusual lipids exploitable as specific biomarkers for their respective diseases. The lipid classes evaluated so far, for the diagnosis of leprosy and tuberculosis, comprise mycolic, mycocerosic and mycolipenic acids with lesser use of members of the phthiocerol family (Figure 2).
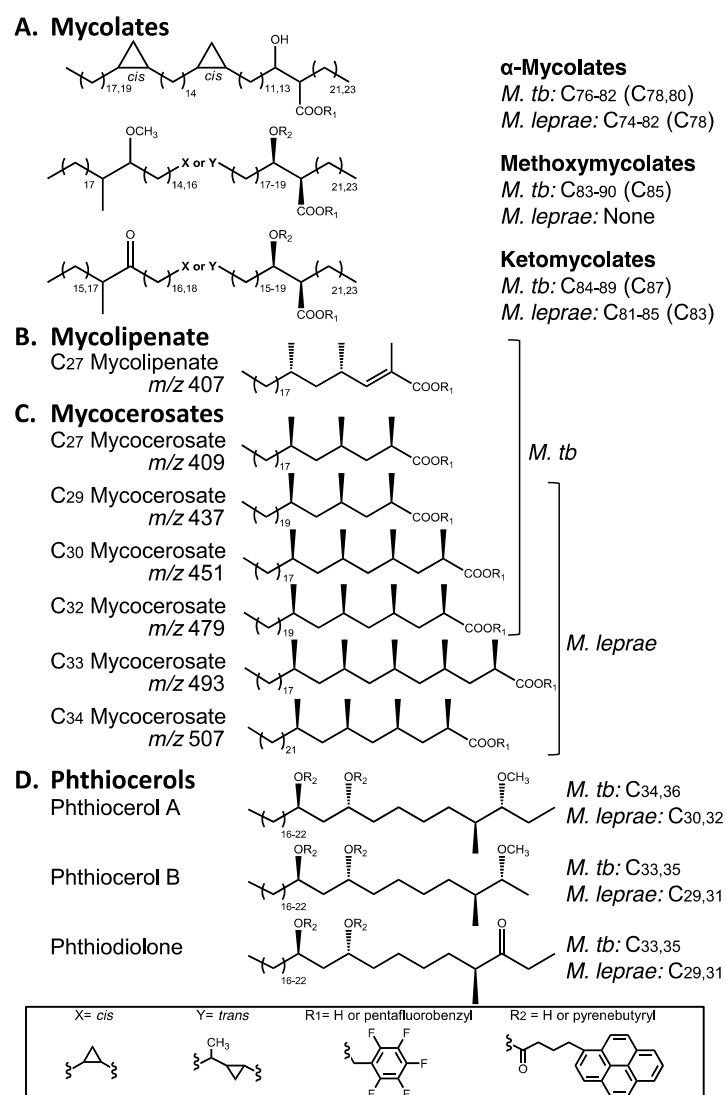

Figure 2. Key lipid biomarker structures for the recognition of ancient tuberculosis and leprosy. (**A**) Mycolic acids, occurring as characteristic homologous types; (**B**) Mycolipenic acid, restricted to the *M. tuberculosis* complex; (**C**) Mycocerosic acids, with C_{34} being particularly diagnostic for leprosy (*m/z* 507, for example, represents the ions observed on GC-MS); (**D**) Phthiocerol family, with distinct size difference between MTB and leprosy.

The characteristic lipid components (Figure 2) of the cell envelopes of *M. tuberculosis* and *M. leprae* are particularly suited for use as disease biomarkers as they are very distinct from all types of mammalian lipids. The 70–90 carbon mycolic acids (Figure 2A) are fatty acids that are four to five times larger than those in mammals that do not generally exceed 20 carbons. Similarly, the 27–34 carbon multi-methyl branched mycolipenic (Figure 2B) and mycocerosic (Figure 2C) acids are readily distinguished. The 29–36 carbon members of the phthiocerol family (Figure 2D) are very distinct mycobacterial biomarkers with no human or animal equivalents. Careful scrutiny of Figure 2 reveals differential distribution of the particular lipid moieties expressed in *M. tuberculosis* and *M. leprae* so that there is the potential to distinguish both diseases, even when they occur in the same specimen. Methods for the exploitation of lipid biomarkers are described below, together with examples that demonstrate their potential.

Initial detection of tuberculosis in archaeological material made use of fluorescence high performance liquid chromatography (HPLC) of anthrylmethyl esters of mycolic acids [9,10,92]. However, the relative instability of these derivatives dictated an alternative approach. An integrated extraction protocol was devised for the extraction of lipid biomarkers and capture of the long-chain acid components as pentafluorobenzyl (PFB) esters [28,29,54]. This allows the analysis of medium-chain C_{24}–C_{34} mycolipenic and mycocerosic acid PFB esters by highly sensitive negative ion chemical ionization (NI-CI) gas chromatography mass spectroscopy (GC-MS) [54]. Stable pyrenebutyric acid (PBA) esters of mycolic acid PFB esters and phthiocerols are prepared (Figure 2) and profiled by fluorescence HPLC using combinations in reverse and normal phase modes [28,29]. Diagnostic certainty can depend on the relative preservation of the particular lipid biomarker classes. If aDNA extraction does not involve organic solvents, lipid biomarkers can be extracted from the residual material [13]. In an isolated Neolithic case, it was possible to characterize MTB mycolic acids by direct mass spectroscopy [63].

3.2. Combined Biomarker Diagnoses—aDNA and Bacterial Cell Wall Lipids

In a pioneering study, detailed mycolic acid profiles, typical of *M. tuberculosis*, supported aDNA fragment amplification to diagnose tuberculosis in ribs from a 1000-year-old skeleton from Addingham, Yorkshire, UK [10]. Similarly, mycolic acids helped confirm tuberculosis in 1400-year-old calcified pleural material from a Byzantine basilica in the Negev desert at Karkur, Israel [9]. A landmark study diagnosed tuberculosis in a ~9 ka woman and child from Atlit-Yam in the Eastern Mediterranean [28]. Distinctive rib lesions were supported by amplification of aDNA and excellent profiles of mycolic and mycocerosic acids [29,66]. The best Atlit-Yam lipid biomarker correlation is shown in Figure 3.

A challenging case was that of "Dr Granville's Egyptian mummy" whose remains are in the British Museum [55]. Resins employed in the mummification process hindered DNA extraction. Nevertheless, *M. tuberculosis* complex DNA was obtained from lung tissue and gall bladder samples, based on nested PCR of the IS*6110* locus. These findings were supported by very good specific *M. tuberculosis* complex cell-wall mycolic acid profiles from lung and femurs demonstrated by HPLC of pyrenebutyric acid–pentafluorobenzyl mycolates. Disseminated tuberculosis may have contributed to the death of the mummified subject. Profiles for Granville mummy femur are illustrated in Figure 4.

Another condition in which combined analyses has proven useful is hypertrophic pulmonary osteoarthropathy (HPO). HPO can be either primary (3% of cases) or more usually secondary to pulmonary, cardiac or abdominal diseases. It is often associated with cancer e.g., brochiogenic tumor, Hodgkin's disease or abdominal neoplasm, but other chronic conditions, such as emphysema, liver cirrhosis or inflammatory bowel disease can lead to HPO. This syndrome consists of clubbing of the digits of the hands and feet, joint inflammation and diffuse sub-periosteal bone deposition. Digital clubbing and joint changes generally involve soft tissue only, so palaeopathological diagnosis of the condition normally depends on the pattern and nature of sub-periosteal bone deposition. The condition is recognized by a diffuse periostitis affecting long bones of the skeleton, distributed in a symmetrical manner [8]. The exact etiology of this condition remains unknown, but is believed to be due to disruption of the ability of the pulmonary capillary bed to degrade circulating factors such as vascular endothelial and platelet derived growth factors.
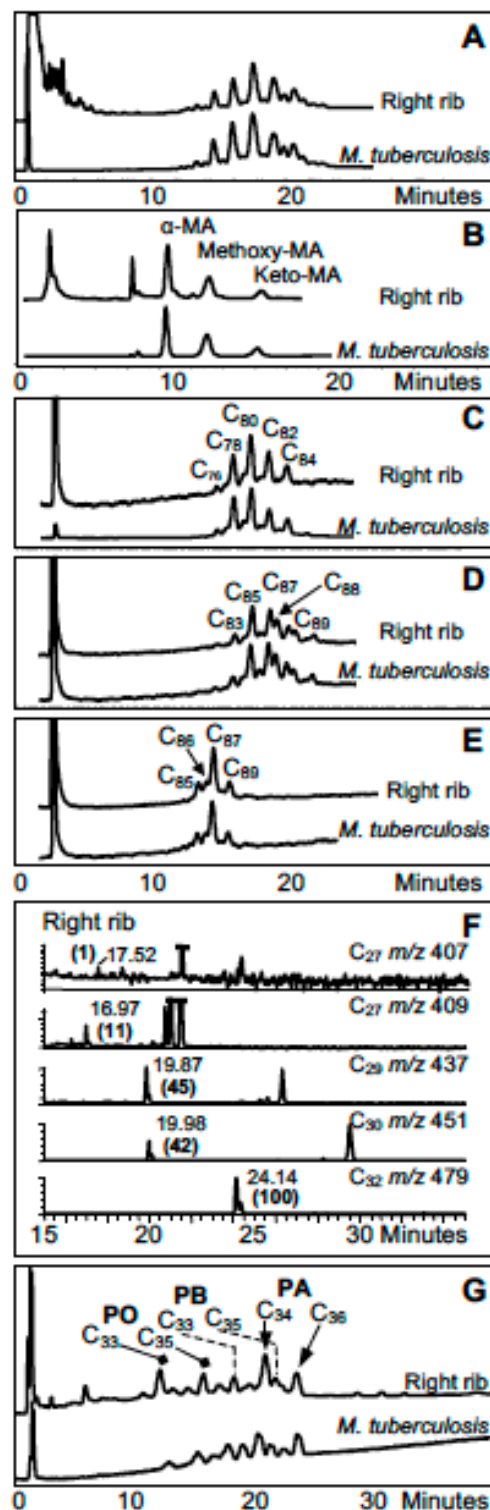
Figure 3. Lipid biomarker profiles for right rib of woman from Atlit-Yam [28,66]. (**A**) Total mycolates, reverse phase high performance liquid chromatography (HPLC); (**B**) Collected total mycolates (MAs), normal phase; (**C**) Collected α-mycolates, reverse phase; (**D**) Collected methoxymycolates, reverse phase; (**E**) Collected ketomycolates, reverse phase; (**F**) Gas chromatography mass spectroscopy (GC-MS) of mycolipenate (C_{27} *m/z* 407) and mycocerosates (C_{27}, C_{29}, C_{30}, C_{32}) characteristic of TB; (**G**) Reverse phase HPLC of phthiocerol family—**PA** phthiocerol A, **PB** phthiocerol B, **PO** phthiodiolone. Comments: Excellent MTB MA and mycocerosate profiles, with weak mycolipenate; good profiles of phthiocerol family. Verdict: Certain MTB.
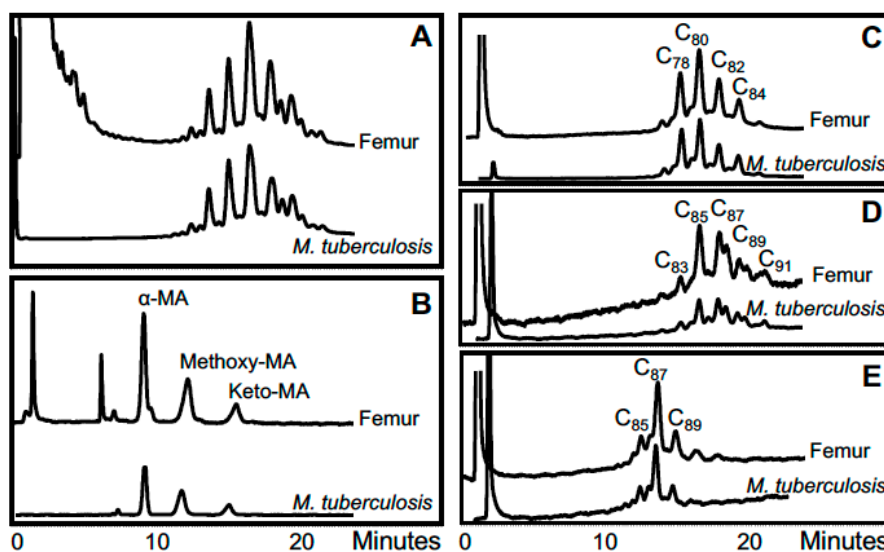
Figure 4. Lipid biomarker profiles for femur of Granville mummy [55]. (**A**) Total mycolates, reverse phase HPLC; (**B**) Collected total mycolates (MAs), normal phase; (**C**) Collected α-mycolates, reverse phase; (**D**) Collected methoxymycolates, reverse phase; (**E**) Collected ketomycolates, reverse phase. Comments: Excellent MTB MA profiles. Verdict: Clear MTB.

An earlier aDNA study, of two cases of HPO from the medieval period (10th–16th century), revealed that infection with *M. tuberculosis* was a likely cause of the condition in one of these individuals, burial EE062 excavated from Wharram Percy [46]. Some years later, the opportunity arose to study a far earlier example of HPO in the 7000-year-old skeleton of a young male individual, body HGO-53, from the Hungarian site of Hódmezövásárhely-Gorzsa. Here, the skeleton presented a case of HPO, with strikingly symmetrical diffuse periostitis on the long bones accompanied with rib changes and cavitations in the vertebral bodies. The palaeopathological diagnosis was HPO secondary to tuberculosis. This was confirmed by aDNA and cell wall lipid analysis. Three of the five skeletons with bone lesions from this site gave supportive weak mycolic acid traces and aDNA, but only HGO-53 was positive in all three biomarker categories, namely mycocerosic and mycolipenic acid derivatives plus IS*1081* PCR [67]. This is a good example of how combinations of different biomarkers can point to a clear consensus that tuberculosis was prevalent in the population under consideration.

In a study of 12 diverse samples from the 10th–19th centuries CE, positive aDNA amplification indicated tuberculosis, leprosy and co-infected cases. However, mycolic acid biomarkers were often quite degraded and discrimination between the various disease conditions was not so evident [12]. In a more extensive survey of twenty 8th century CE skeletons from Bélmegyer-Csömöki domb, Hungary, evidence for *M. tuberculosis* complex aDNA was found in five graves only [75]. Mycolic acid biomarkers were absent in five cases, and the weak, degraded profiles for the remainder were inconclusive for either tuberculosis or leprosy. The most positive lipid biomarker evidence for tuberculosis was provided by mycolipenic acid, with 13 clear cases, supported by five weaker possible cases. Combinations of mycocerosic acids were present in all but three graves and in one case a tuberculosis-leprosy co-infection was indicated. Two specimens with pathology gave no lipid biomarker evidence, but one of these provided *M. tuberculosis* complex DNA fragments. Again, taking together the overall findings, clear evidence of tuberculosis and some leprosy was provided, even though there were no perfect individual cases.

The best evidence for the oldest *Homo sapiens* TB is contained in the ~9 ka Atlit-Yam skeletons (Figure 3), but older cases from the pre-animal domestication phase—Dja'de el Mughara, Northern Syria (10.8–10.3 ka)—and early domestication—Tell Aswad, Southern Syria, (10.2–9.6 ka)—are evident [64]. In the former case, TB aDNA amplification was achieved for individual 483, supported

by clear C_{32} mycocerosates in both a rib and a vertebra. The vertebra also had a convincing signal for mycolipenate offering strong evidence for MTB. Three Tell Aswad fibulae were strong for mycolipenate, weak for mycocerosates, but no aDNA fragments were amplified [64].

The oldest case of amplified aDNA, characteristic of the *M. tuberculosis* complex, was identified in a metacarpal from the Pleistocene ~17 ka *Bison antiquus* recovered from Natural Trap Cave, Wyoming, USA [45]. The aDNA analyses confirmed the *M. tuberculosis* complex, but excluded assignment to modern *M. bovis*. This potentially ground breaking result required confirmatory support and this was provided by lipid biomarkers [29]. The mycolic acid profiles were very weak but extremely strong results were recorded for mycocerosates and particularly for mycolipenate, which is found only in members of the *M. tuberculosis* complex [93]. The combination of lipid biomarkers for the ~17 ka bison is summarized in Figure 5.
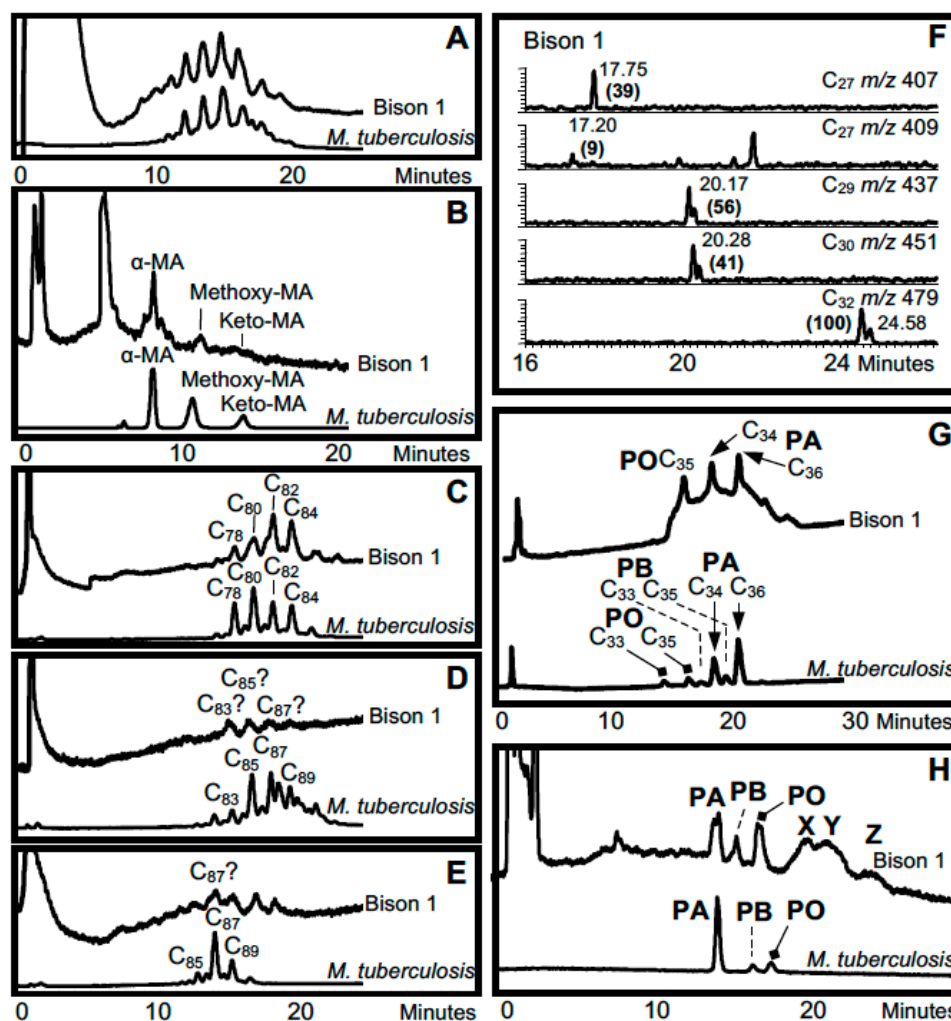

Figure 5. Lipid biomarker profiles for bison metacarpal from Natural Trap Cave with lesions [29,66]. (**A**) Total mycolates, reverse phase HPLC; (**B**) Collected total mycolates, normal phase; (**C**) Collected α-mycolates, reverse phase; (**D**) Collected methoxymycolates, reverse phase; (**E**) Collected ketomycolates, reverse phase; (**F**) GC-MS of mycolipenate (C_{27} *m/z* 407) and mycocerosates (C_{27}, C_{29}, C_{30}, C_{32}) characteristic of TB; (**G**) Reverse phase HPLC of phthiocerol family—**PA** phthiocerol A, **PB** phthiocerol B, **PO** phthiodiolone; (**H**) Normal phase HPLC of collected phthiocerol fraction, **X–Z** are unidentified. Comments: Inconclusive degraded MA profiles, but strong mycolipenate and mycocerosates; positive profiles of phthiocerol family and potentially diagnostic unknowns (**X–Z**). Verdict: Mycolipenate decisively confirms MTB complex.

The choice of this particular bison metacarpal was dictated by the presence of a pronounced lesion "undermining the articular surface". Such metapodial lesions correlate with lesions in human tuberculosis and they are widespread in Pleistocene megafauna including a range of bovids [94] and mastodons [95]. The key validation of the ~17 ka bison lesions, provided by the aDNA and lipid biomarkers, opened up the possibility that tuberculosis infected many megafauna in the Pleistocene [29,96,97].

In the search for ancient leprosy, *M. leprae* aDNA was amplified from skull and tibia fragments from a female skeleton from Uzbekistan, dating to between the 1st and 4th centuries [11]. Genotyping showed this to be a type 3 L, not previously found in archaeological samples. In support, mycolic acids profiles from the skull specimen corresponded well with those from standard *M. leprae*, but only a weak degraded profile was recovered from the tibia sample for both the α-mycolate and ketomycolate fractions [11]. Comprehensive results were obtained for a number of skeletons recovered from St. Mary Magdalen, situated just to the east of Winchester, UK [38]. This *leprosarium* is thought to have been an early Norman foundation, established sometime between 1070 and 1090 CE. This institution survived the Reformation in the 16th century but was used increasingly less for the care of those afflicted with leprosy by that time. In nine excavated individuals, showing skeletal signs of leprosy from the earlier period (10th–12th centuries CE), we were able to amplify *M. leprae* aDNA and in five cases the DNA preservation was sufficient to allow detailed genotyping to be achieved, using single-nucleotide polymorphism (SNP) and multiple locus variable number tandem repeat analysis (MLVA). Three of these best cases (Sk2, Sk7 and Sk19) were assigned to SNP type 3I-1 and the other two (Sk8 and Sk14) to SNP type 2F, with distinct geographical distribution. At the time this study was undertaken, this was the first demonstration of a type 2 strain in the British Isles. Extant examples of strains type 2F have been reported in Turkey and Iran and other type 2s in Nepal (type 2G), Ethiopia (type 2H) and Malawi (type 2E) [18]. The significant diversity of amplified aDNA is complemented by the uniform foundation of the mycolate and mycocerosate lipid biomarker profiles that correspond well with those of *M. leprae*. The power of the combined biomarker data is illustrated in Figure 6 for representative Winchester skeleton Sk2 (type 3I-1); the mycocerosate data are unpublished (O.Y-C. Lee, H.H.T. Wu, G.M. Taylor, K. Tucker, R. Butler, S. Roffey, P. Marter, D.E. Minnikin, G.S. Besra, G.R. Stewart; manuscript in preparation).

This coherent research laid the basis for progression to the first full exploitation of full genomics of ancient leprosy cases using WGS techniques [39]. Along with three Scandinavian specimens (3077 from Sigtuna Sweden; Refshale 16 from Denmark and Jorgen 625 from Denmark), this pioneering study included Winchester Sk2 and Sk8 and confirmed and expanded the findings initially obtained by the conventional approaches of PCR and Sanger sequencing. The excellent preservation of aDNA at the Winchester site, possibly assisted by the location of many burials beneath *leprosaria* buildings that persisted over hundreds of years, resulted in two further whole genome retrievals in a later work, which concentrated on the less studied, type 2F strains [74]. The prevalence of these type 2 strains here indicates that they may have been the co-dominant at this location during the 11th century in contrast to later European and associated North American type 3I isolates.

A particularly informative and early case is a 4th–6th century CE male skeleton from Great Chesterford, Essex, UK. Both multi- and single copy loci from the *M. leprae* genome were obtained after aDNA amplification. An ancestral variant of the type 3I-1 lineage was found [40]. Mycolic acid profiles were somewhat degraded with no discernible signals for ketomycolates. Strong α-mycolate traces for metatarsal and talus specimens were recorded but the main components were 2 carbons less than that usually found for standard *M. leprae*. However, excellent profiles of mycocerosates typical of *M. leprae* were recorded. Complementary aDNA and lipid biomarker data for a metatarsal sample are shown in Figure 7. At present, this case of leprosy is the earliest radiocarbon dated case in Britain confirmed by both aDNA and lipid biomarkers.
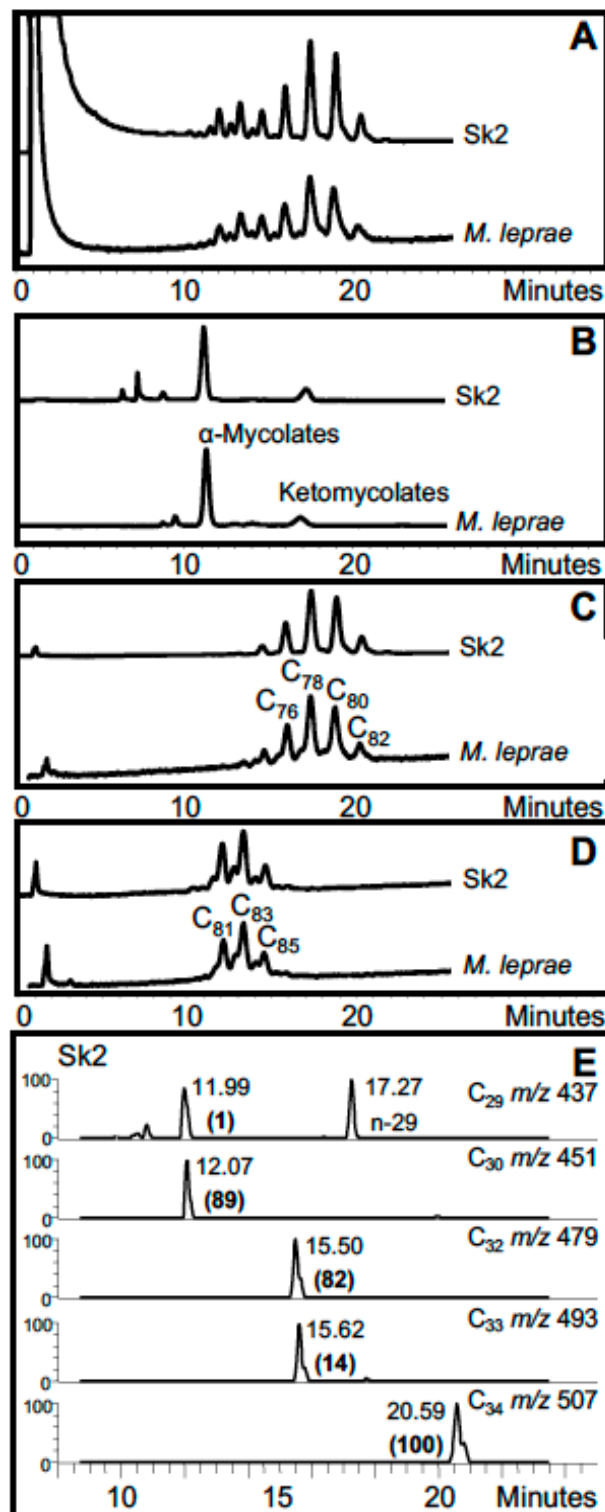
Figure 6. Lipid biomarker profiles for Winchester leprosy specimen Sk2 [38]. (**A**) Total mycolates, reverse phase HPLC; (**B**) Collected total mycolates (MAs), normal phase; (**C**) Collected α-mycolates, reverse phase; (**D**) Collected ketomycolates, reverse phase; (**E**) GC-MS of mycocerosates (C_{29}, C_{30}, C_{32}, C_{33}, C_{34}) characteristic of leprosy. Comments: Excellent leprosy MA and mycocerosate profiles. Verdict: Certain leprosy.
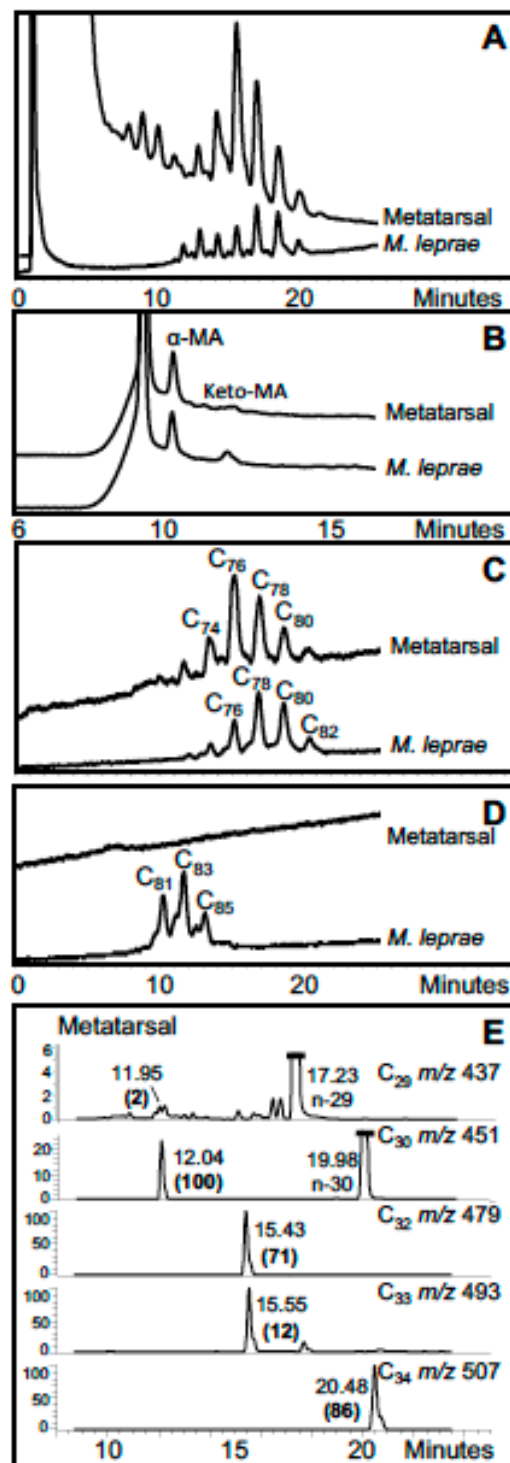
Figure 7. Lipid biomarker profiles for metatarsal from Great Chesterford leprosy specimen GC 96 [40]. (**A**) Total mycolates, reverse phase HPLC; (**B**) Collected total mycolates (MAs), normal phase; (**C**) Collected α-mycolates, reverse phase; (**D**) Collected ketomycolates, reverse phase; (**E**) GC-MS of mycocerosates (C_{29}, C_{30}, C_{32}, C_{33}, C_{34}) characteristic of leprosy. Comments: Inconclusive degraded MA profile has α-mycolates four carbons shorter than *M. leprae,* but good mycocerosate profile has *M. leprae*-specific C_{34} mycocerosate. Verdict: Most likely leprosy and not MTB.

In an extensive survey of the spread of ancient leprosy in Europe, two specimens from a young adult female (18 R and 18 L), and a specimen from a slightly older male (144)—all from 7th century CE Vicenne, Italy—gave consistent but unusual mycolic acid profiles with α-mycolates that had four-fewer carbons. However, 18R and 18L gave clear *M. leprae* mycocerosate profiles, correlating with aDNA amplification; no aDNA was recovered from specimen 144 but a weak, recognizable mycocerosate profile was recorded [14].

In addition to defining individual ancient cases of tuberculosis and leprosy, aDNA fragment amplification and lipid biomarker detection has excellent potential for unraveling mixed infection cases. A particular skeleton (KD 517) from a 7th–8th century CE site at Kiskundorozsma, Hungary, provided aDNA amplicons for both tuberculosis and leprosy [13]. Fortuitously, the key points of the mycolate and mycocerosate profiles were clear enough to enable a rough ratio of lipid biomarkers for tuberculosis to leprosy of 3:2 to be estimated. This is an exemplary informative case as the initial bone pathology suggested only leprosy. The lipid biomarker results are shown in Figures 8 and 9. Joint cases of ancient tuberculosis and leprosy have been encountered in several other studies (Table 2, Table S2).
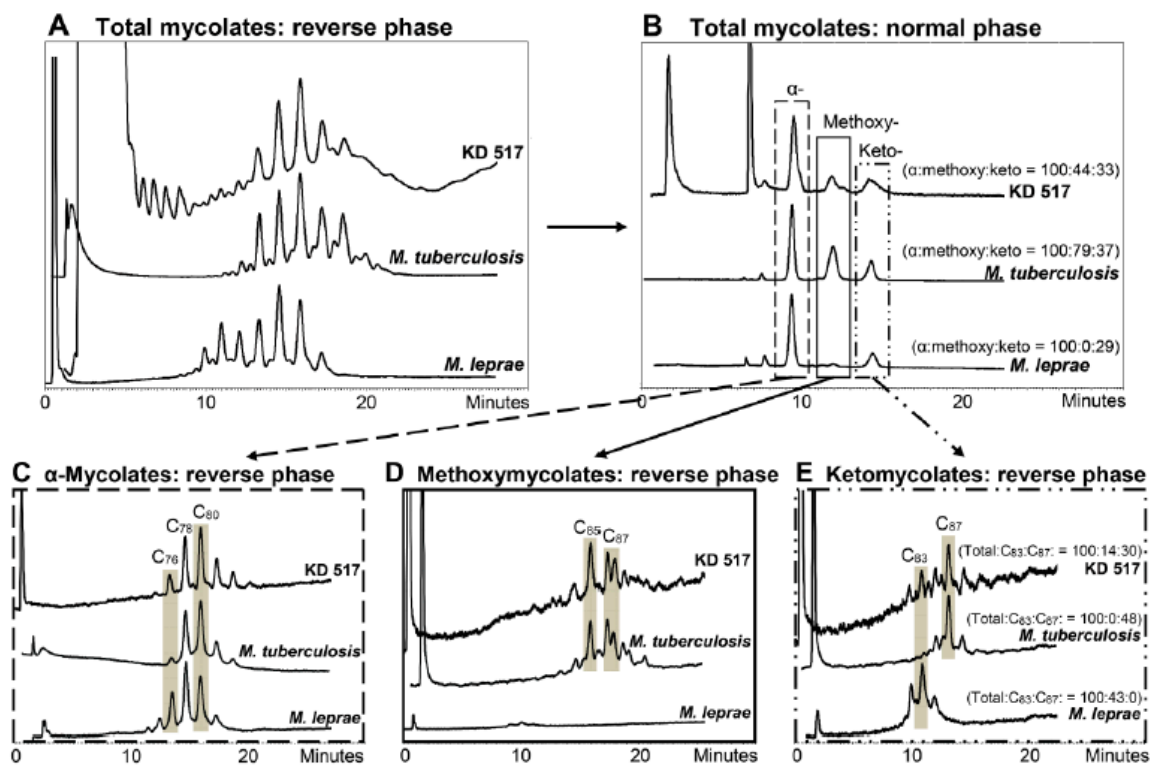
Figure 8. Mycolic acid profiles from Kiskundorozsma, Hungary, KD 517 [13]. (**A**) Total mycolates, reverse phase HPLC. (**B**) Collected total mycolates (MAs), normal phase; the normalized ratios of the α-mycolates, methoxymycolates and ketomycolates, respectively, are in brackets. (**C**–**E**): Reverse phase HPLC of collected α-mycolate, methoxymycolate and ketomycolate fractions, respectively; the normalized ratios of ketomycolate C_{83} and C_{87} components are shown in brackets in (**E**). Comments: Good total MA profile (**A**) and α-mycolates (**C**) resemble MTB, but ketomycolates (**E**) have a C_{83} component typical of *M. leprae*. Verdict: Major MTB with inconclusive indication of leprosy.

Figure 9. Mycocerosic acid GC-MS profiles from extracts of KD 517 [13] (**A**) KD 517. (**B**) *M. tuberculosis*. (**C**) *M. leprae*. Comments: Good mycocerosate profi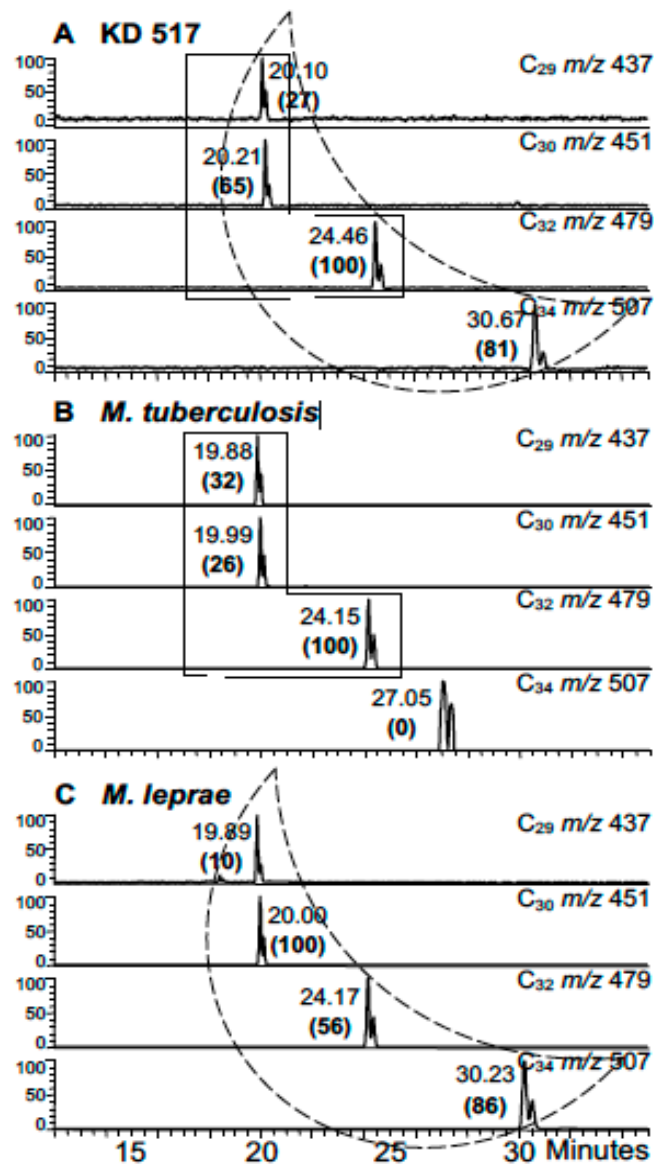le has *M. leprae*-specific C_{34} mycocerosate; a search for mycolipenate might have helped confirm MTB. The C_{34} component at 27.05 min in the *M. tuberculosis* standard (**B**) is not a mycocerosate. Verdict: Mycocerosates confirm some leprosy, but mycolate profiles (Figure 8) show predominance of MTB.

4. The Authenticity and Validity of aDNA and Lipid Biomarkers for Ancient Tuberculosis and Leprosy

The earliest indications of tuberculosis and leprosy were characteristic changes in bone morphology [8,98,99]. As summarized above, the introduction of amplification of diagnostic aDNA fragments gave immediate reinforcement of the recognition of ancient TB and leprosy (Tables 1 and 2), thereby providing a solid foundation for the study of ancient mycobacterial disease. Confirmation of these diagnoses has been increasingly supported by the detection of key lipid biomarkers, providing overall confidence in the published conclusions. Of particular importance were the landmark studies of human TB from Atlit-Yam [28] and megafaunal TB from Natural Trap Cave [29,45]. In both cases, initial aDNA amplification was conclusively reinforced by pristine lipid biomarker profiles (Figures 3 and 5). Nevertheless, there remains a persistent undercurrent of subjective opinion that denies the validity

of this pioneering, objectively reviewed body of work. There are examples where aDNA findings are criticized yet strong supportive evidence from lipid biomarkers is ignored [100,101], and doubts thus raised tend to persist, in spite of detailed published rebuttals [102,103]. Alternatively, the potential of lipid biomarker evidence may be acknowledged [104] but the only citation is an independent review of non-nucleotide biomarkers [105], ignoring any of the well-documented original studies [28,29,55].

Dismissal of clear combined aDNA and lipid biomarker evidence is particularly noticeable in cases where extrapolations of genomic data point to a particular date for the most recent common ancestor (MRCA) of TB. A very original study [32] showed that pre-Columbian TB in Peru was due to *Mycobacterium pinnepedii*, probably acquired from seals. However, the authors extrapolated limited genomic data to propose that TB was only about 6000 years old. Their overall conclusion was interpreted to exclude all reports of ancient TB older than ~6 ka, yet no citations of such studies were provided. Their exclusion criteria [32] are quoted below:

(1) "rate heterogeneity or horizontal gene transfer is obscuring our dating analysis, perhaps as a result of human population expansions which increase the availability of susceptible hosts and allow selection to operate more quickly,

(2) the pathogens identified in the earlier archaeological material are in fact not members of the MTBC, but rather are ancestral forms that have since undergone replacements, or

(3) certain techniques for MTBC identification in archaeological material lack specificity."

The first statement, (1) is a simple let-out clause, suggesting a possible lack of validity in the assumptions on which their conclusions are based. Similarly, the third criterion (3) does not require detailed comment as the "certain techniques" are not specified and the results of any such techniques have nevertheless been peer reviewed and validly published [93,96,106].

The second criterion, (2), depends on a clear definition of what is encompassed by the MTBC concept and some clarification is warranted. The identified 6 ka MRCA [32] may indeed be a "replacement" but this does not mean that the strains that were replaced, did not cause tuberculosis, and could not be included in the broad taxon labelled *M. tuberculosis*. The complex issue of evolving clonal bacterial populations has been addressed in detail, as represented in Figure 10 [107].

Key pertinent guidelines from the perceptive overview of Smith *et al.* (2009) [107] (Figure 10) are quoted below.

(1) "Every species has a most recent common ancestor (MRCA) that is the coalescence of all extant lineages. The MRCA of *M. tuberculosis* is not necessarily the first strain of *M. tuberculosis* to infect humans, and is no more than the coalescence of all extant lineages; it may have been one member of a large population of *M. tuberculosis* strains (Figure 10)".

(2) "The MRCA of *M. tuberculosis*, or any species, can change over time as lineages die out and the population evolves (Figure 10). The MRCA of a population is based on the sum of all extant strains, and if lineages become extinct then the MRCA will change. Both selective sweeps (the replacement of all alleles in a population by a selected allele) and drift (the random loss of lineages from a population by sampling each generation) can cause lineages to become extinct. For example, if Beijing strains of *M. tuberculosis* outcompete all other extant lineages then the MRCA of all extant *M. tuberculosis* strains will become a Beijing strain. This change in the MRCA of a species is common to all organisms, but is probably more important for clonal organisms such as *M. tuberculosis*, for which selective sweeps can drive whole chromosomes to fixation and purge all variation in the population."

(3) "*M. tuberculosis* may have infected humans for hundreds of thousands of years, or longer, before the current MRCA appeared, but those ancient lineages have been lost from the present population. Thus, molecular dating does not tell us how long humans and *M. tuberculosis* have coexisted (Figure 10)".
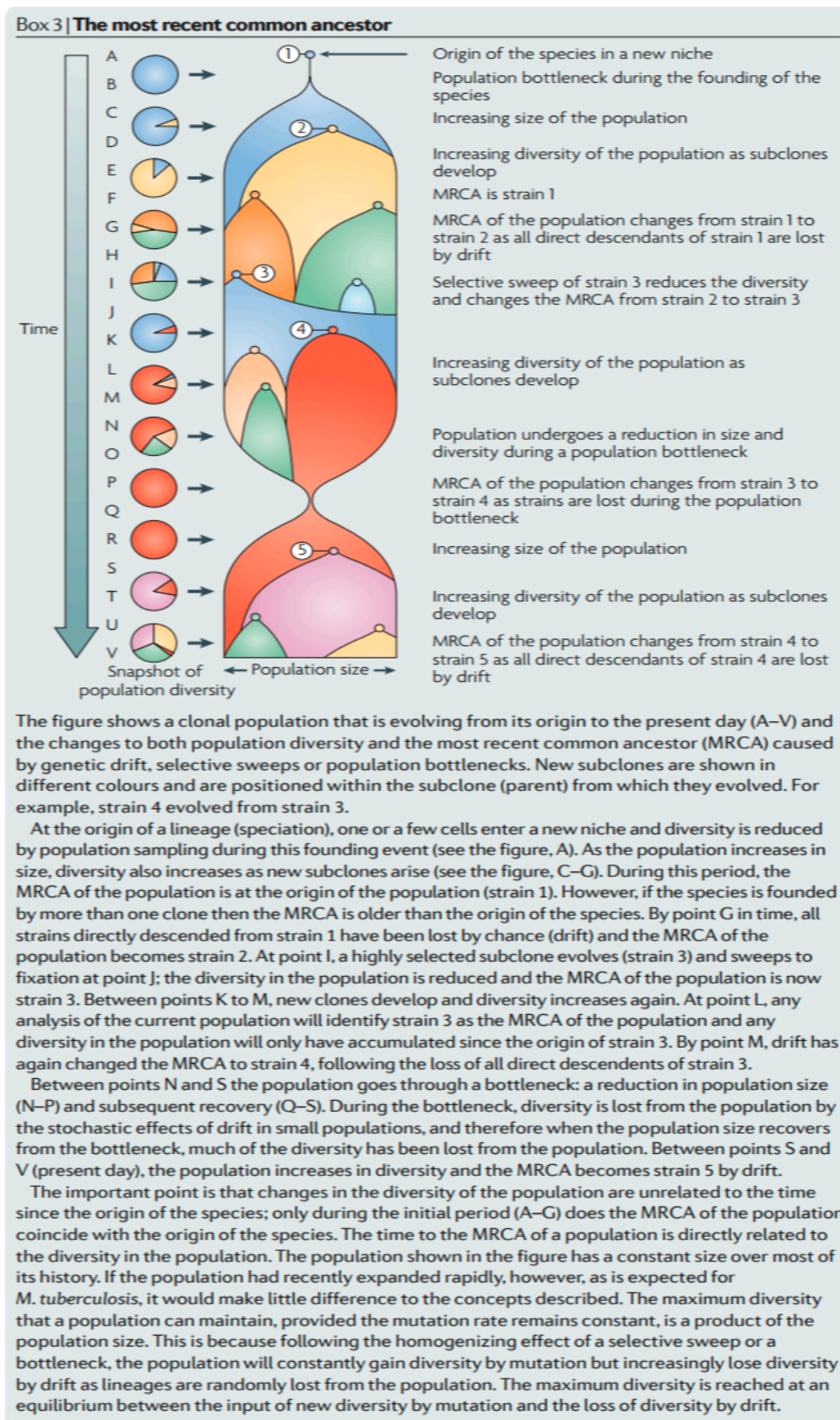
Box 3 | The most recent common ancestor

① Origin of the species in a new niche

Population bottleneck during the founding of the species

Increasing size of the population

② Increasing diversity of the population as subclones develop

MRCA is strain 1

MRCA of the population changes from strain 1 to strain 2 as all direct descendants of strain 1 are lost by drift

③ Selective sweep of strain 3 reduces the diversity and changes the MRCA from strain 2 to strain 3

④ Increasing diversity of the population as subclones develop

Population undergoes a reduction in size and diversity during a population bottleneck

MRCA of the population changes from strain 3 to strain 4 as strains are lost during the population bottleneck

⑤ Increasing size of the population

Increasing diversity of the population as subclones develop

MRCA of the population changes from strain 4 to strain 5 as all direct descendants of strain 4 are lost by drift

The figure shows a clonal population that is evolving from its origin to the present day (A–V) and the changes to both population diversity and the most recent common ancestor (MRCA) caused by genetic drift, selective sweeps or population bottlenecks. New subclones are shown in different colours and are positioned within the subclone (parent) from which they evolved. For example, strain 4 evolved from strain 3.

At the origin of a lineage (speciation), one or a few cells enter a new niche and diversity is reduced by population sampling during this founding event (see the figure, A). As the population increases in size, diversity also increases as new subclones arise (see the figure, C–G). During this period, the MRCA of the population is at the origin of the population (strain 1). However, if the species is founded by more than one clone then the MRCA is older than the origin of the species. By point G in time, all strains directly descended from strain 1 have been lost by chance (drift) and the MRCA of the population becomes strain 2. At point I, a highly selected subclone evolves (strain 3) and sweeps to fixation at point J; the diversity in the population is reduced and the MRCA of the population is now strain 3. Between points K to M, new clones develop and diversity increases again. At point L, any analysis of the current population will identify strain 3 as the MRCA of the population and any diversity in the population will only have accumulated since the origin of strain 3. By point M, drift has again changed the MRCA to strain 4, following the loss of all direct descendants of strain 3.

Between points N and S the population goes through a bottleneck: a reduction in population size (N–P) and subsequent recovery (Q–S). During the bottleneck, diversity is lost from the population by the stochastic effects of drift in small populations, and therefore when the population size recovers from the bottleneck, much of the diversity has been lost from the population. Between points S and V (present day), the population increases in diversity and the MRCA becomes strain 5 by drift.

The important point is that changes in the diversity of the population are unrelated to the time since the origin of the species; only during the initial period (A–G) does the MRCA of the population coincide with the origin of the species. The time to the MRCA of a population is directly related to the diversity in the population. The population shown in the figure has a constant size over most of its history. If the population had recently expanded rapidly, however, as is expected for *M. tuberculosis*, it would make little difference to the concepts described. The maximum diversity that a population can maintain, provided the mutation rate remains constant, is a product of the population size. This is because following the homogenizing effect of a selective sweep or a bottleneck, the population will constantly gain diversity by mutation but increasingly lose diversity by drift as lineages are randomly lost from the population. The maximum diversity is reached at an equilibrium between the input of new diversity by mutation and the loss of diversity by drift.

Figure 10. An objective general overview of most recent common ancestors (MRCAs) [107].

A simplified interpretation of the above detailed statements is provided by reference to the hypothetical graphical picture presented in Figure 10 [107]. The suggested MTB MRCA at ~6 ka, derived by molecular dating [32], could correspond, for example, to the strain labelled ⑤ in Figure 10. However, access to direct ancestors of mycobacteria, corresponding to point ⑤, has been lost by genetic drift. Earlier populations, represented by strain ④ are still *M. tuberculosis* but they may be currently inaccessible from reference genomes, such as those used to postulate the ~6 ka MRCA [32]. As indicated in Figure 10, a representative strain, such as ④, could have co-existed with strain ⑤ and caused tuberculosis practically up to the present day. Care must be taken, therefore, not to consider strains of evolving pathogens in strict chronological order, as potential ancestors (e.g., ④) of accessible strains (e.g., ⑤) may not have become immediately extinct. A possibly related informative example of this phenomenon concerns the diverse taxon comprised of smooth tubercle bacilli, labelled *"Mycobacterium canettii"* [96,97]. Relatives of *"M. canettii"* are likely ancestors of the MTB complex but they are occasionally isolated from current tuberculosis patients [96,97]. It is clear, therefore, that an absolute age of ~6 ka cannot be imposed for tubercle bacilli, as fully endorsed elsewhere in a detailed review [108]. The above arguments are also relevant for a more recent restatement of a ~6 ka TB age limit [33].

The supposed ~6 ka TB MCRA limit has been subjectively relaxed in a recent review, but still the authenticity of any older cases remain denied [109]. The dogmatic view continues, that anything short of a full genome is unacceptable. This sustained subjective denial of the value of aDNA amplification [109] also totally and conveniently ignores the solid body of lipid biomarker evidence for landmark cases, such as the ~9ka Atlit-Yam woman and child (Figure 3) [28] and the ~17 ka bison (Figure 5) [29]. Indeed, deliberately ignoring ancient lipid data is tacit evidence of the value of these biomarkers that are difficult to dismiss on contamination grounds as no amplification is involved. Detection of ancient disease should be a purely forensic operation, all evidence being admissible. All-inclusive genomic evidence may be conclusive but failing that, a diagnostic portfolio can be assembled from combinations of established factors, such as bone lesions, aDNA and lipid biomarkers. Combinations of evidence are then judged by peer review and authoritative publications are added to the record. The identification of ancient leprosy by aDNA fragment amplification, occasionally supported by lipid biomarkers, has not been subjected to the same level of subjective scrutiny as ancient tuberculosis even though the analytical protocols are practically identical. The power of the general approach is amply illustrated by the example of the jointly infected specimen KD 517 where amplicons for both TB and leprosy were detected and the non-amplified lipid profiles were clear enough to allow estimates of the bacterial load for each disease (Figures 8 and 9).

A perspective on past investigations and future capabilities for ancient TB is illustrated in Figure 11. Currently it is apparent that full TB genomics have only reached back a few thousand years, but aDNA amplification of degraded fragments has allowed diagnoses of ancient disease at least to 17 ka [45]. Lipid biomarkers have also easily reached this 17 ka landmark in a bison metacarpal (Figure 5) [29]. The overall age of tuberculosis remains undefined but the limits of current techniques (Figure 11) may be stretched and new approaches may be developed to reach even further into the past.
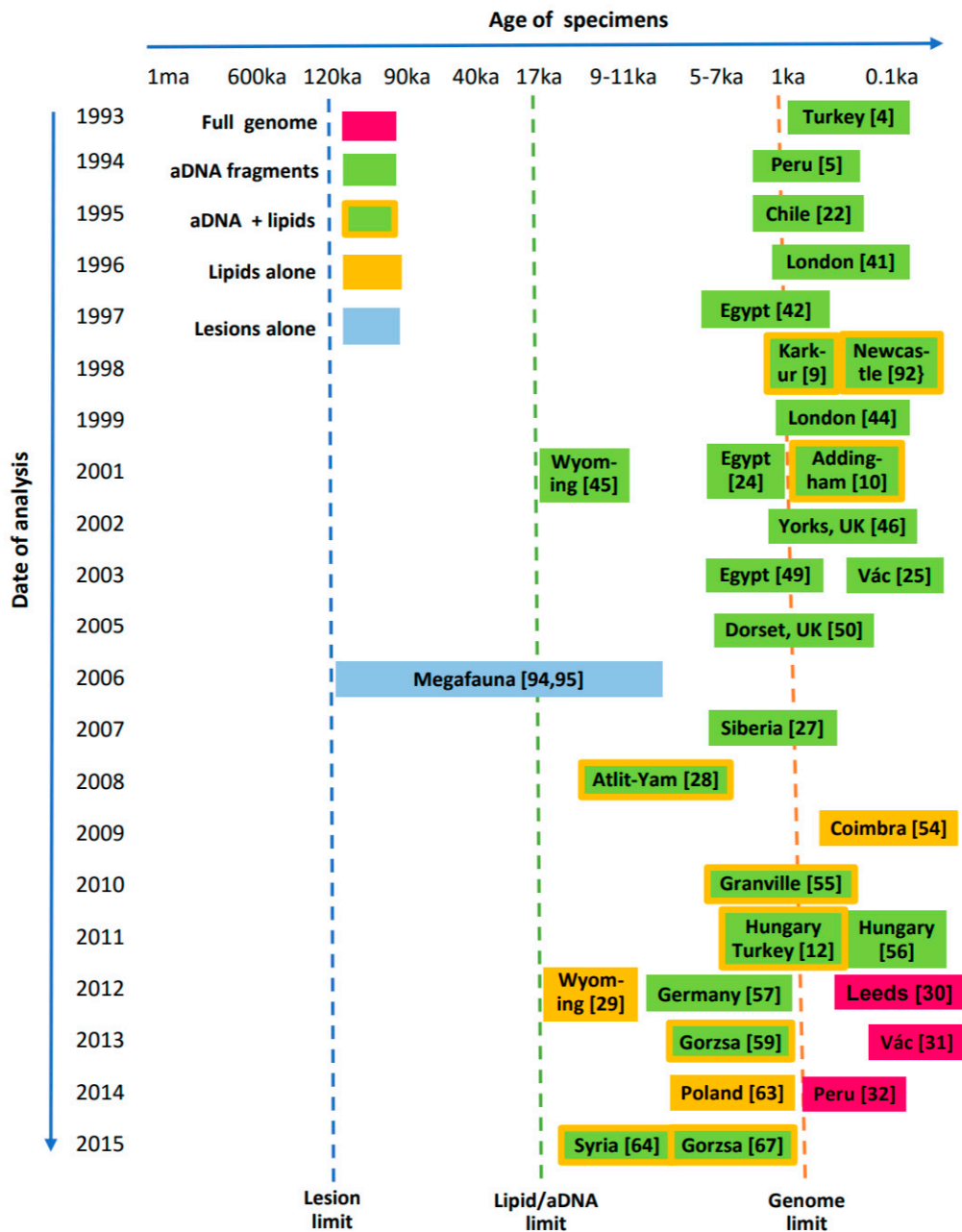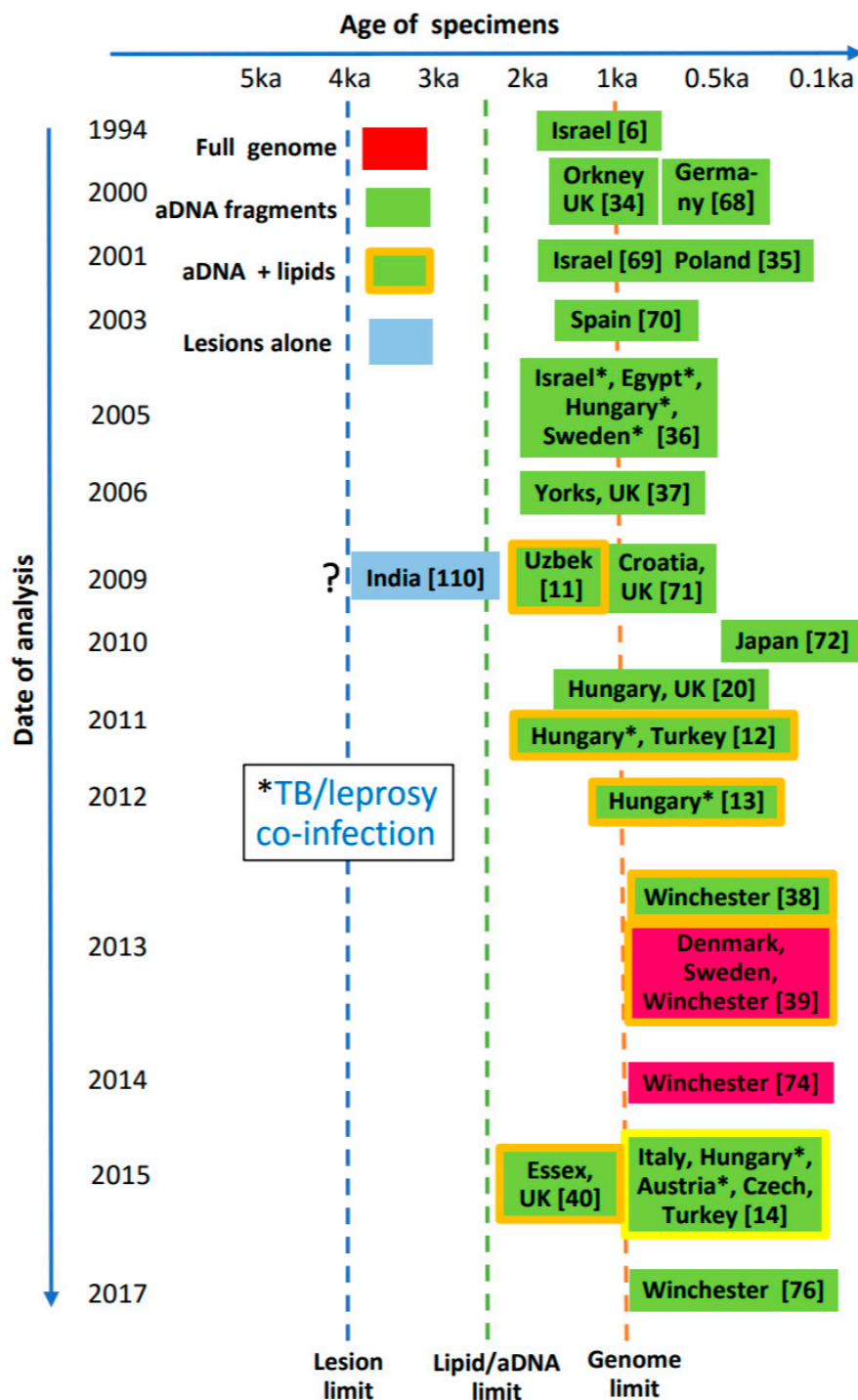
Figure 11. Interrelation between age of suspected ancient tuberculosis specimens and dates of various analytical investigations. Vertical dotted lines show current limits for diagnostic techniques.

In contrast, evidence for ancient leprosy does not appear to stretch back more than several thousand years (Figure 12). The oldest skeletal indication appears to be a specimen from India, dated at around 2000 BCE [110]. Currently, the most ancient leprosy genomes have been recovered from mediaeval European cases [39,74]. A number of joint leprosy/MTB cases are also highlighted in Figure 12.

Figure 12. Interrelation of age of suspected ancient leprosy specimens and dates of various analytical investigations. Vertical dotted lines show current limits for diagnostic techniques. The Indian specimen [110] represents the oldest known case with lesions indicative of leprosy, but requires validation.

5. Conclusions

The fields of aDNA amplification and lipid biomarker analysis have been systematically developed over the last two decades to produce significant contributions to our understanding of the host-pathogen interactions of the ancient diseases of leprosy and tuberculosis. Both techniques assist osteologists in the confirmation of disease in human or animal remains, particularly in incomplete

or damaged skeletons or in the early stage of disease when lesions may be inconclusive. Thus they may assist with differential diagnosis in situations such as lytic vertebral lesions that could be due either to Pott's disease of the spine or brucellosis. They can identify cases where co-infections may be present. These techniques can document the prevalence of disease in past populations and highlight specific links with human activity such as farming and proximity to zoonoses such as *M. bovis*. On occasion, ancient DNA or lipid biomarkers can identify novel or alleged palaeopathological indicators of disease, for example periostitic rib lesions and HPO as indicators of pulmonary tuberculosis.

The greater stability of some lipid biomarkers, such as mycolic, mycolipenic and mycocerosic acids, increases the chances for successful detection of mycobacterial disease in older cases where aDNA has not survived. Conventional genotyping and recent advances with WGS extend our knowledge of the diversity and spread of both mycobacterial pathogens, at least in recent times. A consequence of the current limited range of a few thousand years for the use of WGS (Figures 10 and 11) is that the deep origins of tuberculosis and leprosy remain obscure. Combinations of aDNA amplification and lipid biomarkers currently provide informative data and signposts for older sources of mycobacterial disease, particularly for tuberculosis back into the Pleistocene epoch.

A current essential strategy, in looking for ancient tuberculosis and leprosy in archaeological materials, should initially involve observation of any physical indications, such as bone lesions. Circumstantial evidence, the presence of leprosaria for example, is also very important. A logical next step would be to attempt to extract good quality aDNA to enable the production of full mycobacterial genomes. Amplification of key aDNA fragments would be a fallback position, ideally with lipid biomarker confirmation. Finally, lipid biomarkers alone can provide evidence for ancient tuberculosis and/or leprosy.

References

1.　World Health Organization. *Global Leprosy Strategy 2016–2020*; Cooreman, E.A., Ed.; Department of Control of Neglected Tropical Diseases, WHO: Geneva, Switzerland, 2016. Available online: www.who.int/lep/resources/9789290225096/en/ (accessed on 31 July 2017).

2.　World Health Organization. Global Tuberculosis Report 2016. Available online: www.who.int/tb/publications/global_report/en/ (accessed on 31 July 2017).

3.　Gagneux, S. Host-pathogen co-evolution in human tuberculosis. *Philos. Trans. R. Soc. B* **2012**, *367*, 850–859. [CrossRef] [PubMed]

4.　Spigelman, M.; Lemma, E. The use of the polymerase chain reaction (PCR) to detect *Mycobacterium tuberculosis* in ancient skeletons. *Int. J. Osteoarchaeol.* **1993**, *3*, 137–143. [CrossRef]

5.　Salo, W.L.; Aufderheide, A.C.; Buikstra, J.; Holcomb, T.A. Identification of *Mycobacterium tuberculosis* DNA in a pre-Columbian Peruvian mummy. *Proc. Natl. Acad. Sci. USA* **1994**, *91*, 2091–2094. [CrossRef] [PubMed]

6.　Rafi, A.; Spigelman, M.; Stanford, J.; Lemma, E.; Donoghue, H.; Zias, J. DNA of *Mycobacterium leprae* detected by PCR in ancient bone. *Int. J. Osteoarchaeol.* **1994**, *4*, 287–290. [CrossRef]

7.　Møller-Christensen, V.; Hughes, D.R. Two early cases of leprosy in Great Britain. *Man* **1962**, *62*, 177–179. [CrossRef]

8.　Ortner, D.J.; Putschar, W.J.G. *Identification of Pathological Conditions in Human Skeletal Remains*; Smithsonian Institution Press: Washington, DC, USA, 1985.

9. Donoghue, H.D.; Spigelman, M.; Zias, J.; Gernaey-Child, A.M.; Minnikin, D.E. *Mycobacterium tuberculosis* complex DNA in calcified pleura from remains 1400 years old. *Lett. Appl. Microbiol.* **1998**, *27*, 265–269. [CrossRef] [PubMed]

10. Gernaey, A.M.; Minnikin, D.E.; Copley, M.S.; Dixon, R.A.; Middleton, J.C.; Roberts, C.A. Mycolic acids and ancient DNA confirm an osteological diagnosis of tuberculosis. *Tuberculosis* **2001**, *81*, 259–265. [CrossRef] [PubMed]

11. Taylor, G.M.; Blau, S.; Mays, S.; Monot, M.; Lee, O.Y.-C.; Minnikin, D.E.; Besra, G.S.; Cole, S.T.; Rutland, P. *Mycobacterium leprae* genotype amplified from an archaeological case of lepromatous leprosy in central Asia. *J. Archaeol. Sci.* **2009**, *36*, 2408–2414. [CrossRef]

12. Minnikin, D.E.; Besra, G.S.; Lee, O.Y.-C.; Spigelman, M.; Donoghue, H.D. The interplay of DNA and lipid biomarkers in the detection of tuberculosis and leprosy in mummies and other skeletal remains. In *Yearbook of Mummy Studies*; Gill-Frerking, H., Rosendahl, W., Zink, A., Piombino-Mascali, D., Eds.; Verlag Dr. Friedrich Pfeil: Munich, Germany, 2011; Volume 1, pp. 109–114.

13. Lee, O.Y.-C.; Bull, I.D.; Molnár, E.; Marcsik, A.; Pálfi, G.; Donoghue, H.D.; Besra, G.S.; Minnikin, D.E. Integrated strategies for the use of lipid biomarkers in the diagnosis of ancient mycobacterial disease. In *the Twelfth Annual Conference of the British Association for Biological Anthropology and Osteoarchaeology, Department of Archaeology and Anthropology, University of Cambridge 2010*; Mitchell, P.D., Buckberry, J., Eds.; Archaeopress: Oxford, UK, 2012; pp. 63–69.

14. Donoghue, H.D.; Taylor, G.M.; Marcsik, A.; Molnár, E.; Pálfi, G.; Pap, I.; Teschler-Nicola, M.; Pinhasi, R.; Erdal, Y.S.; Velemínsky, P.; et al. A migration-driven model for the historical spread of leprosy in medieval Eastern and Central Europe. *Infect. Genet. Evol.* **2015**, *31*, 250–256. [CrossRef] [PubMed]

15. Gagneux, S.; DeRiemer, K.; Van, T.; Kato-Maeda, M.; de Jong, B.C.; Narayanan, S.; Nicol, M.; Niemann, S.; Kremer, K.; Gutierrez, M.C.; et al. Variable host-pathogen compatibility in *Mycobacterium tuberculosis*. *Proc. Natl. Acad. Sci. USA* **2006**, *108*, 2869–2873. [CrossRef] [PubMed]

16. Maiden, M.C.J. Putting leprosy on the map. *Nature Genet.* **2009**, *41*, 1264–1266. [CrossRef] [PubMed]

17. Monot, M.; Honoré, N.; Garnier, T.; Araoz, R.; Coppée, J.-Y.; Lacroix, C.; Sow, S.; Spencer, J.S.; Truman, R.W.; Williams, D.L.; et al. On the origin of leprosy. *Science* **2005**, *308*, 1040–1042. [CrossRef] [PubMed]

18. Monot, M.; Honoré, N.; Garnier, T.; Zidane, N.; Sherafi, D.; Paniz-Mondolfi, A.; Matsuoka, M.; Taylor, G.M.; Donoghue, H.D.; Bouwman, A.; et al. Comparative genomic and phylogeographic analysis of *Mycobacterium leprae*. *Nature Genet.* **2009**, *41*, 1282–1289. [CrossRef] [PubMed]

19. Sreevatsan, S.; Pan, X.; Stockbauer, K.E.; Connell, N.D.; Krieswirth, B.N.; Whittam, T.S.; Musser, J.M. Restricted structural gene polymorphism in the *Mycobacterium tuberculosis* complex indicates evolutionarily recent global dissemination. *Proc. Natl. Acad. Sci. USA* **1997**, *94*, 9869–9874. [CrossRef] [PubMed]

20. Taylor, G.M.; Donoghue, H.D. Multiple loci variable number tandem repeat (VNTR) analysis (MLVA) of *Mycobacterium leprae* isolates amplified from European archaeological human remains with lepromatous leprosy. *Microb. Infect.* **2011**, *13*, 923–929. [CrossRef] [PubMed]

21. Kamerbeek, J.; Schouls, L.; Kolk, A.; van Agterveld, M.; van Soolingen, D.; Kuijper, S.; Bunschoten, A.; Molhuizen, H.; Shaw, R.; Goyal, M.; et al. Simultaneous detection and strain differentiation of *Mycobacterium tuberculosis* for diagnosis and epidemiology. *J. Clin. Microbiol.* **1997**, *35*, 907–914. [PubMed]

22. Arrieza, B.T.; Salo, W.; Aufderheide, A.C.; Holcomb, T.A. Pre-Columbian tuberculosis in northern Chile: Molecular and skeletal evidence. *Am. J. Phys. Anthropol.* **1995**, *98*, 37–45. [CrossRef] [PubMed]

23. Baron, H.; Hummel, S.; Herrmann, B. *Mycobacterium tuberculosis* complex DNA in ancient human bones. *J. Archaeol. Sci.* **1996**, *23*, 667–671. [CrossRef]

24. Zink, A.; Haas, C.J.; Reischl, U.; Szeimies, U.; Nerlich, A.G. Molecular analysis of skeletal tuberculosis in an ancient Egyptian population. *J. Med. Microbiol.* **2001**, *50*, 355–366. [CrossRef] [PubMed]

25. Fletcher, H.A.; Donoghue, H.D.; Holton, J.; Pap, I.; Spigelman, M. Widespread occurrence of *Mycobacterium tuberculosis* DNA from 18th–19th century Hungarians. *Am. J. Phys. Anthropol.* **2003**, *120*, 144–152. [CrossRef] [PubMed]

26. Bathurst, R.R.; Barta, J.L. Molecular evidence of tuberculosis induced hypertrophic osteopathy in a 16th century Iroquoian dog. *J. Archaeol. Sci.* **2004**, *31*, 917–925. [CrossRef]

27. Taylor, G.M.; Murphy, E.; Hopkins, R.; Rutland, P.; Chistov, Y. First report of *Mycobacterium bovis* DNA in human remains from the Iron Age. *Microbiology* **2007**, *153*, 1243–1249. [CrossRef] [PubMed]

28. Hershkovitz, I.; Donoghue, H.D.; Minnikin, D.E.; Besra, G.S.; Lee, O.Y.-C.; Gernaey, A.M.; Galili, E.; Eshed, V.; Greenblatt, C.L.; Lemma, E.; et al. Detection and molecular characterization of 9000-year-old *Mycobacterium tuberculosis* from a Neolithic settlement in the eastern Mediterranean. *PLoS ONE* **2008**, *3*, e3426. [CrossRef] [PubMed]

29. Lee, O.Y.-C.; Wu, H.H.T.; Donoghue, H.D.; Spigelman, M.; Greenblatt, C.L.; Bull, I.D.; Rothschild, B.M.; Martin, L.D.; Minnikin, D.E.; Besra, G.S. *Mycobacterium tuberculosis* complex lipid virulence factors preserved in the 17,000-year-old skeleton of an extinct bison, *Bison antiquus*. *PLoS ONE* **2012**, *7*, e41923. [CrossRef] [PubMed]

30. Bouwman, A.S.; Kennedy, S.L.; Müller, R.; Stephens, R.H.; Holst, M.; Caffell, A.C.; Roberts, C.A.; Brown, T.A. Genotype of a historic strain of *Mycobacterium tuberculosis*. *Proc. Natl. Acad. Sci. USA* **2012**, *109*, 18511–18516. [CrossRef] [PubMed]

31. Chan, J.Z.-M.; Sergeant, M.J.; Lee, O.Y.-C.; Minnikin, D.E.; Besra, G.S.; Pap, I.; Spigelman, M.; Donoghue, H.D.; Pallen, M.J. Metagenomic analysis of tuberculosis in a mummy. *N. Engl. J. Med.* **2013**, *369*, 289–290. [CrossRef] [PubMed]

32. Bos, K.I.; Harkins, K.M.; Herbig, A.; Coscolla, M.; Weber, N.; Comas, I.; Forrest, S.A.; Bryant, J.M.; Harris, S.R.; Schuenemann, V.J.; et al. Pre-Columbian mycobacterium genomes reveal seals as a source of New World human tuberculosis. *Nature* **2014**, *514*, 494–497. [CrossRef] [PubMed]

33. Kay, G.L.; Sergeant, M.J.; Zhou, Z.; Chan, J.Z.-M.; Millard, A.; Quick, J.; Szikossy, I.; Pap, I.; Spigelman, M.; Loman, N.J.; et al. Eighteenth-century genomes show that mixed infections were common at time of peak tuberculosis in Europe. *Nature Comms.* **2015**, *6*, 6717. [CrossRef] [PubMed]

34. Taylor, G.M.; Widdison, S.; Brown, I.N.; Young, D. A mediaeval case of lepromatous leprosy from 13th–14th century Orkney, Scotland. *J. Archaeol. Sci.* **2000**, *27*, 1133–1138. [CrossRef]

35. Donoghue, H.D.; Holton, J.; Spigelman, M. PCR primers that can detect low levels of *Mycobacterium leprae* DNA. *J. Med. Microbiol.* **2001**, *50*, 177–182. [CrossRef] [PubMed]

36. Donoghue, H.D.; Marcsik, A.; Matheson, C.; Vernon, K.; Nuorala, E.; Molto, J.E.; Greenblatt, C.L.; Spigelman, M. Co-infection of *Mycobacterium tuberculosis* and *Mycobacterium leprae* in human archaeological samples: A possible explanation for the historical decline of leprosy. *Proc. R. Soc. B* **2005**, *272*, 389–394. [CrossRef] [PubMed]

37. Taylor, G.M.; Watson, C.L.; Bouwman, A.S.; Lockwood, D.N.; Mays, S.A. Variable number tandem repeat (VNTR) typing of two palaeopathological cases of lepromatous leprosy from mediaeval England. *J. Archaeol. Sci.* **2006**, *33*, 1569–1579. [CrossRef]

38. Taylor, G.M.; Tucker, K.; Butler, R.; Pike, A.W.G.; Lewis, J.; Roffey, S.; Marter, P.; Lee, O.Y.-C.; Wu, H.H.T.; Minnikin, D.E.; et al. Detection and strain typing of ancient *Mycobacterium leprae* from a medieval leprosy hospital. *PLoS ONE* **2013**, *8*, e62406. [CrossRef] [PubMed]

39. Schuenemann, V.J.; Singh, P.; Mendum, T.A.; Krause-Kyora, B.; Jäger, G.; Bos, K.I.; Herbig, A.; Economou, C.; Benjak, A.; Busso, P.; et al. Genome-wide comparison of medieval and modern *Mycobacterium leprae*. *Science* **2013**, *341*, 179–183. [CrossRef] [PubMed]

40. Inskip, S.A.; Taylor, G.M.; Zakrzewski, S.R.; Mays, S.A.; Pike, A.W.G.; Llewellyn, G.; Williams, C.M.; Lee, O.Y.-C.; Wu, H.H.T.; Minnikin, D.E.; et al. Osteological, biomolecular and geochemical examination of an early Anglo-Saxon case of lepromatous leprosy. *PLoS ONE* **2015**, *10*, e0124282. [CrossRef] [PubMed]

41. Taylor, G.M.; Crossey, M.; Saldanha, J.; Waldron, T. DNA from *Mycobacterium tuberculosis* identified in mediaeval human skeletal remains using polymerase chain reaction. *J. Archaeol. Sci.* **1996**, *23*, 789–798. [CrossRef]

42. Nerlich, A.G.; Haas, C.J.; Zink, A.; Szeimies, U.; Hagedorn, H.G. Molecular evidence for tuberculosis in an ancient Egyptian mummy. *Lancet* **1997**, *350*, 1404. [CrossRef]

43. Braun, M.; Collins Cook, D.; Pfeiffer, S. DNA from *Mycobacterium tuberculosis* complex identified in North America, pre-Columbian human skeletal remains. *J. Archaeol. Sci.* **1998**, *25*, 271–277. [CrossRef]

44. Taylor, G.M.; Goyal, M.; Legge, A.J.; Shaw, R.J.; Young, D. Genotypic analysis of *Mycobacterium tuberculosis* from medieval human remains. *Microbiology* **1999**, *145*, 899–904. [CrossRef] [PubMed]

45. Rothschild, B.M.; Martin, L.D.; Lev, G.; Bercovier, H.; Kahila Bar-Dal, G.; Greenblatt, C.; Donoghue, H.; Spigelman, M.; Brittain, D. *Mycobacterium tuberculosis* complex DNA from an extinct bison dated 17,000 years before the present. *Clin. Infect. Dis.* **2001**, *33*, 305–311. [CrossRef] [PubMed]

46. Mays, S.; Taylor, G.M. Osteological and biomolecular study of two possible cases of hypertrophic osteoarthropathy from mediaeval England. *J. Archaeol. Sci.* **2002**, *29*, 1267–1276. [CrossRef]

47. Spigelman, M.; Matheson, C.; Lev, G.; Greenblatt, C.; Donoghue, H.D. Confirmation of the presence of *Mycobacterium tuberculosis* complex-specific DNA in three archaeological specimens. *Int. J. Osteoarchaeol.* **2002**, *12*, 393–401. [CrossRef]

48. Taylor, G.M.; Stewart, G.R.; Cooke, M.; Chaplin, S.; Ladva, S.; Kirkup, J.; Palmer, S.; Young, D.B. Koch's bacillus—A look at the first isolate of *Mycobacterium tuberculosis* from a modern perspective. *Microbiology* **2003**, *149*, 3213–3220. [CrossRef] [PubMed]

49. Zink, A.R.; Sola, C.; Reischl, U.; Grabner, W.; Rastogi, N.; Wolf, H.; Nerlich, A.G. Characterization of *Mycobacterium tuberculosis* complex DNAs from Egyptian mummies by spoligotyping. *J. Clin. Microbiol.* **2003**, *41*, 359–367. [CrossRef] [PubMed]

50. Taylor, G.M.; Young, D.B.; Mays, S.A. Genotypic analysis of the earliest known prehistoric case of tuberculosis in Britain. *J. Clin. Microbiol.* **2005**, *45*, 2236–2240. [CrossRef] [PubMed]

51. Spigelman, M.; Pap, I.; Donoghue, H.D. A death from Langerhans cell histiocytosis and tuberculosis in 18th century Hungary—What palaeopathology can tell us today. *Leukemia* **2006**, *20*, 740–742. [CrossRef] [PubMed]

52. Matheson, C.D.; Vernon, K.K.; Lahti, A.; Fratpietro, R.; Spigelman, M.; Gibson, S.; Greenblatt, C.L.; Donoghue, H.D. Molecular exploration of the first-century *Tomb of the Shroud* in Akeldama, Jerusalem. *PLoS ONE* **2009**, *4*, e8319. [CrossRef] [PubMed]

53. Murphy, E.M.; Chistov, Y.K.; Hopkins, R.; Rutland, P.; Taylor, G.M. Tuberculosis among Iron Age individuals from Tyva, South Siberia: Palaeopathological and biomolecular findings. *J. Archaeol. Sci.* **2009**, *36*, 2029–2038. [CrossRef]

54. Redman, J.E.; Shaw, M.J.; Mallet, A.I.; Santos, A.L.; Roberts, C.A.; Gernaey, A.M.; Minnikin, D.E. Mycocerosic acid biomarkers for the diagnosis of tuberculosis in the Coimbra skeletal collection. *Tuberculosis* **2009**, *89*, 267–277. [CrossRef] [PubMed]

55. Donoghue, H.D.; Lee, O.Y.-C.; Minnikin, D.E.; Besra, G.S.; Taylor, J.H.; Spigelman, M. Tuberculosis in Dr Granville's mummy: A molecular re-examination of the earliest known Egyptian mummy to be scientifically examined and given a medical diagnosis. *Proc. R. Soc. B* **2010**, *277*, 51–56. [CrossRef] [PubMed]

56. Donoghue, H.D.; Pap, I.; Szikossy, I.; Spigelman, M. Detection and characterization of *Mycobacterium tuberculosis* DNA in 18th century Hungarians with pulmonary and extra-pulmonary tuberculosis. In *Yearbook of Mummy Studies*; Gill-Frerking, H., Rosendahl, W., Zink, A., Piombino-Mascali, D., Eds.; Verlag Dr. Friedrich Pfeil: Munich, Germany, 2011; Volume 1, pp. 51–56.

57. Nicklisch, N.; Maixner, F.; Gansimeier, R.; Friederich, S.; Dresely, V.; Meller, H.; Zink, A.; Alt, K.W. Rib lesions in skeletons from early Neolithic sites in central Germany: on the trail of tuberculosis at the onset of agriculture. *Am. J. Phys. Anthropol.* **2012**, *149*, 391–404. [CrossRef] [PubMed]

58. Corthals, A.; Koller, A.; Martin, D.W.; Rieger, R.; Chen, E.I.; Bernaski, M.; Recagno, G.; Dávalos, L.M. Detecting the immune system response of a 500 year-old Inca mummy. *PLoS ONE* **2012**, *7*, e41244. [CrossRef] [PubMed]

59. Masson, M.; Molnár, E.; Donoghue, H.D.; Besra, G.S.; Minnikin, D.E.; Wu, H.H.T.; Lee, O.Y.-C.; Bull, I.; Pálfi, G. Osteological and biomolecular evidence of a 7000-year-old case of hypertrophic pulmonary osteopathy secondary to tuberculosis from Neolithic Hungary. *PLoS ONE* **2013**, *8*, e78252. [CrossRef] [PubMed]

60. Lairemruata, A.; Ball, M.; Bianucci, R.; Weite, B.; Nerlich, A.G.; Kun, J.F.J.; Putsch, C.M. Molecular identification of falciparum malaria and human tuberculosis co-infections in mummies from the Fayum Depression (Lower Egypt). *PLoS ONE* **2013**, *8*, e60307.

61. Dabernat, H.; Thèves, C.; Bouakaze, C.; Nikolaeva, D.; Keyser, C.; Mokrousov, I.; Géraut, A.; Duchesne, S.; Gérard, P.; Alexeev, A.N.; et al. Tuberculosis epidemiology and selection in an autochthonous Siberian population from the 16th–19th century. *PLoS ONE* **2013**, *9*, e89877. [CrossRef] [PubMed]

62. Müller, R.; Roberts, C.A.; Brown, T.A. Biomolecular identification of ancient *Mycobacterium tuberculosis* complex DNA in human remains from Britain and continental Europe. *Am. J. Phys. Anthropol.* **2014**, *153*, 178–189. [CrossRef] [PubMed]

63. Boroska-Strugińska, B.; Druszczyńska, M.; Lorkiewicz, W.; Szewczyk, R.; Żądzińska, E. Mycolic acids as markers of osseous tuberculosis in the Neolithic skeleton from Kujawy region (central Poland). *Anthropol. Rev.* **2014**, *77*, 137–149.

64. Baker, O.; Lee, O.Y.-C.; Wu, H.H.T.; Besra, G.S.; Minnikin, D.E.; Llewellyn, G.; Williams, C.M.; Maixner, F.; O'Sullivan, N.; Zink, A.; et al. Human tuberculosis predates domestication in ancient Syria. *Tuberculosis* **2015**, *95*, S4–S12. [CrossRef] [PubMed]

65. Hershkovitz, I.; Donoghue, H.D.; Minnikin, D.E.; May, H.; Lee, O.Y.-C.; Feldman, M.; Galili, E.; Spigelman, M.; Rothschild, B.M.; Kahila Bar-Gal, G. Tuberculosis origin: The Neolithic scenario. *Tuberculosis* **2015**, *95*, S122–S126. [CrossRef] [PubMed]

66. Lee, O.Y.-C.; Wu, H.H.T.; Besra, G.S.; Rothschild, B.M.; Spigelman, M.; Hershkovitz, I.; Kahila Bar-Gal, G.; Donoghue, H.D.; Minnikin, D.E. Lipid biomarkers provide evolutionary signposts for the oldest known cases of tuberculosis. *Tuberculosis* **2015**, *95*, S127–S132. [CrossRef] [PubMed]

67. Masson, M.; Bereczki, Z.; Molnár, E.; Donoghue, H.D.; Minnikin, D.E.; Lee, Y.-C.; Wu, H.H.T.; Besra, G.S.; Bull, I.D.; Pálfi, G. 7000 year-old tuberculosis cases from Hungary—Osteological and biomolecular evidence. *Tuberculosis* **2015**, *95*, S13–S17. [CrossRef] [PubMed]

68. Haas, C.J.; Zink, A.; Pálfi, G.; Szeimies, U.; Nerlich, A.G. Detection of leprosy in ancient human skeletal remains by molecular identification of *Mycobacterium leprae*. *Am. J. Clin. Pathol.* **2000**, *114*, 428–436. [CrossRef] [PubMed]

69. Spigelman, M.; Donoghue, H.D. Brief communication: Unusual pathological condition in the lower extremities of a skeleton from ancient Israel. *Am. J. Phys. Anthropol.* **2001**, *114*, 92–93. [CrossRef]

70. Montiel, R.; García, C.; Cañadas, M.P.; Isidro, A.; Guijo, J.M.; Malgosa, A. DNA sequences of *Mycobacterium leprae* recovered from ancient bones. *FEMS Microbiol. Lett.* **2003**, *226*, 413–414. [CrossRef]

71. Watson, C.L.; Popescu, E.; Boldsen, J.; Slaus, M.; Lockwood, D.N. Single nucleotide polymorphism analysis of European archaeological *M. leprae* DNA. *PLoS ONE* **2009**, *4*, e7547. [CrossRef] [PubMed]

72. Suzuki, K.; Takigawa, W.; Tanigawa, K.; Nakamura, K.; Ishido, Y.; Kawashima, A.; Wu, H.; Akama, T.; Sue, M.; Yoshihara, A.; et al. Detection of *Mycobacterium leprae* DNA from archaeological skeletal remains in Japan using whole genome amplification and polymerase chain reaction. *PLoS ONE* **2010**, *5*, e12422. [CrossRef] [PubMed]

73. Economou, C.; Kjellström, A.; Lidén, K.; Panagopoulos, I. Ancient-DNA reveals an Asian type of *Mycobacterium leprae* in medieval Scandinavia. *J. Archaeol. Sci.* **2013**, *40*, 465–470, Corrigendum, p. 2867. [CrossRef]

74. Mendum, T.A.; Schuenemann, V.J.; Roffey, S.; Taylor, G.M.; Wu, H.; Singh, P.; Tucker, K.; Hinds, J.; Cole, S.T.; Kierzek, A.M.; et al. *Mycobacterium leprae* genomes from a British medieval leprosy hospital: Towards understanding an ancient epidemic. *BMC Genomics* **2014**, *15*, 270. [CrossRef] [PubMed]

75. Molnár, E.; Donoghue, H.D.; Lee, O.Y.-C.; Wu, H.H.T.; Besra, G.S.; Minnikin, D.E.; Bull, I.D.; Llewellyn, G.; Williams, C.M.; Spekker, O.; et al. Morphological and biomolecular evidence for tuberculosis in 8th century AD skeletons from Bélmegyer-Csömöki domb, Hungary. *Tuberculosis* **2015**, *95*, S35–S41.

76. Roffey, S.; Tucker, K.; Filipek-Ogden, K.; Montgomery, J.; Cameron, J.; O'Connell, T.; Evans, J.; Marter, J.; Taylor, G.M. Investigation of a medieval pilgrim burial excavated from the *leprosarium* of St Mary Magdalen Winchester, UK. *PLoS Negl. Trop. Dis.* **2017**, *11*, e0005186. [CrossRef] [PubMed]

77. Spigelman, M.; Donoghue, H.D. Palaeobacteriology with special reference to pathogenic bacteria. In *Emerging Pathogens: The Archaeology, Ecology, and Evolution of Infectious Disease*; Greenblatt, C.L., Spigelman, M., Eds.; Oxford University Press Inc.: New York, NY, USA, 2003; pp. 175–188.

78. Poinar, H.N.; Hofreiter, M.; Spauding, W.G.; Martin, P.S.; Stankiewicz, B.A.; Bland, H.; Evershed, R.P.; Possnert, G.; Pääbo, S. Molecular coproscopy: Dung and diet of the extinct ground sloth *Nothrotheriops shastensis*. *Science* **1998**, *281*, 402–406. [CrossRef] [PubMed]

79. Boom, R.; Sol, C.J.; Salimans, M.M.; Jansen, C.L.; Wertheim-van Dillen, P.M.; van der Noordaa, J. Rapid and simple method for purification of nucleic acids. *J. Clin. Microbiol.* **1990**, *28*, 495–503. [PubMed]

80. Bouwman, A.S.; Brown, T.A. Comparison between silica-based methods for the extraction of DNA from human bones from 18th to mid-19th century London. *Ancient Biomol.* **2002**, *4*, 173–178. [CrossRef]

81. Abu Al-Soud, W.; Rådström, P. Effects of amplification facilitators on diagnostic PCR in the presence of blood, feces, and meat. *J. Clin. Microbiol.* **2000**, *38*, 4463–4470. [PubMed]

82. Cano, R.J. Analysing ancient DNA. *Endeavour* **1996**, *20*, 162–167. [CrossRef]

83. Telenti, A.; Imboden, P.; Marchesi, F.; Lowrie, D.; Cole, S.; Colston, M.J.; Matter, L.; Schopfer, K.; Bodmer, T. Detection of rifampicin-resistance mutations in *Mycobacterium tuberculosis*. *J. Clin. Microbiol.* **1993**, *31*, 175–178. [CrossRef]

84. Mays, S.; Taylor, G.M.; Legge, A.J.; Young, D.B.; Turner-Walker, G. Am. J. Paleopathological and biomolecular study of tuberculosis in a medieval skeletal collection from England. *Am. J. Phys. Anthropol.* **2001**, *114*, 298–311. [CrossRef] [PubMed]

85. Mostowy, S.; Inwald, J.; Gordon, S.; Martin, C.; Warren, R.; Kremer, K.; Cousins, D.; Behr, M.A. Revisiting the evolution of *Mycobacterium bovis*. *J. Bacteriol.* **2005**, *187*, 6386–6395. [CrossRef] [PubMed]

86. Young, S.K.; Taylor, G.M.; Jain, S.; Suneetha, L.M.; Suneetha, S.; Lockwood, D.N.J.; Young, D.B. Microsatellite mapping of *Mycobacterium leprae* populations in infected humans. *J. Clin. Microbiol.* **2004**, *42*, 4931–4936. [CrossRef] [PubMed]

87. Zhang, L.; Budiaswan, T.; Matsuoka, M. Diversity of potential short tandem repeats in *Mycobacterium leprae* and application for molecular typing. *J. Clin. Microbiol.* **2005**, *43*, 5221–5229. [CrossRef] [PubMed]

88. Supply, P.; Allix, C.; Lesjean, S.; Cardoso-Oelemann, M.; Rüsch-Gerdes, S.; Willery, E.; Savine, E.; de Haas, P.; van Deutekon, H.; Roring, S.; et al. Proposal for standardization of optimized mycobacterial interspersed repetitive unit-variable-number tandem repeat typing of *Mycobacterium tuberculosis*. *J. Clin. Microbiol.* **2006**, *44*, 4498–4510. [CrossRef] [PubMed]

89. Smith, N.H.; Dale, J.; Inwald, J.; Palmer, S.I.; Gordon, S.V.; Hewinson, R.G.; Maynard Smith, J. The population structure of *Mycobacterium bovis* in Great Britain: Clonal expansion. *Proc. Natl. Acad. Sci. USA* **2003**, *100*, 15271–15275. [CrossRef] [PubMed]

90. Lovett, S.T. Encoded errors: Mutations and rearrangements mediated by misalignment at repetitive DNA sequences. *Mol. Microbiol.* **2004**, *52*, 1243–1253. [CrossRef] [PubMed]

91. Taylor, G.M. Ancient DNA and the fingerprints of disease: Retrieving human pathogen genomic sequences from archaeological remains using real-time quantitative polymerase chain reaction. In *Molecular Diagnostics; Current Research and Applications*; Huggett, J., O'Grady, J., Eds.; Caister Academic Press: Haverhill, Suffolk, UK, 2014; pp. 115–137. ISBN 978-1-908230-41-6.

92. Gernaey, A.M.; Minnikin, D.E.; Copley, M.S.; Power, J.J.; Ahmed, A.M.S.; Dixon, R.A.; Roberts, C.A.; Robertson, D.J.; Nolan, J.; Chamberlain, A. Detecting ancient tuberculosis. *Internet Archaeol.* **1998**, *5*. [CrossRef]

93. Minnikin, D.E.; Lee, O.Y.-C.; Wu, H.H.T.; Nataraj, V.; Donoghue, H.D.; Ridell, M.; Watanabe, M.; Alderwick, L.; Bhatt, A.; Besra, G.S. Pathophysiological implications of cell envelope structure in *Mycobacterium tuberculosis* and related taxa. In *Tuberculosis—Expanding Knowledge*; Ribon, W., Ed.; Intech: Rijeka, Croatia, 2015; pp. 145–175. ISBN 978-953-51-2139-8.

94. Rothschild, B.M.; Martin, L.D. Did ice-age bovids spread tuberculosis? *Naturwissenschaften* **2006**, *11*, 565–569. [CrossRef] [PubMed]

95. Rothschild, B.M.; Laub, R. Hyperdisease in the late Pleistocene: validation of an early 20th century hypothesis. *Naturwissenschaften* **2006**, *11*, 557–564. [CrossRef] [PubMed]

96. Minnikin, D.E.; Lee, O.Y.-C.; Wu, H.H.T.; Besra, G.S.; Bhatt, A.; Nataraj, V.; Rothschild, B.M.; Spigelman, M.; Donoghue, H.D. Ancient mycobacterial lipids: Key reference biomarkers in charting the evolution of tuberculosis. *Tuberculosis* **2015**, *95*, S133–S139. [CrossRef] [PubMed]

97. Jankute, M.; Nataraj, V.; Lee, O.Y.-C.; Wu, H.H.T.; Ridell, M.; Garton, N.J.; Barer, M.R.; Minnikin, D.E.; Bhatt, A.; Besra, G.S. The role of hydrophobicity in tuberculosis evolution and pathogenicity. *Sci. Rep.* **2017**, *7*, 1315. [CrossRef] [PubMed]

98. Møller-Christensen, V.; Weiss, D.L. One of the oldest datable skeletons with leprous bone-changes from the Naestved leprosy hospital churchyard in Denmark. *Int. J. Lepr.* **1971**, *39*, 172–182.

99. Holloway, K.L.; Henneberg, R.J.; de Barros Lopes, M.; Henneberg, M. Evolution of human tuberculosis: A systematic review and meta-analysis of paleopathological evidence. *HOMO J. Comp. Hum. Biol.* **2011**, *62*, 402–458. [CrossRef] [PubMed]

100. Stone, A.C.; Wilbur, A.K.; Buikstra, J.E.; Roberts, C.A. Tuberculosis and leprosy in perspective. *Yearbk. Phys. Anthropol.* **2009**, *52*, 66–94. [CrossRef] [PubMed]

101. Wilbur, A.K.; Bouwman, A.S.; Stone, A.C.; Roberts, C.A.; Pfister, L.-A.; Buikstra, J.E.; Brown, T.A. Deficiencies and challenges in the study of ancient tuberculosis DNA. *J. Archaeol. Sci.* **2009**, *36*, 1990–1997. [CrossRef]

102. Donoghue, H.D.; Hershkovitz, I.; Minnikin, D.E.; Besra, G.S.; Lee, O.Y.-C.; Galili, E.; Greenblatt, C.L.; Lemma, E.; Spigelman, M.; Kahila Bar-Gal, G. Biomolecular archaeology of ancient tuberculosis: Response to "Deficiencies and challenges in the study of ancient tuberculosis DNA" by Wilbur et al. (2009). *J. Archaeol. Sci.* **2009**, *36*, 2797–2804. [CrossRef]

103. Taylor, G.M.; Mays, S.A.; Huggett, J.F. Ancient DNA (aDNA) studies of man and microbes: General similarities, specific differences. *Int. J. Osteoarchaeol.* **2010**, *20*, 747–751. [CrossRef]

104. Harkins, K.M.; Stone, A.C. Ancient pathogen genomics: insights into timing and adaptation. *J. Hum. Evol.* **2015**, *79*, 137–149. [CrossRef] [PubMed]

105. Tran, T.-N.-N.; Aboudharam, G.; Raoult, D.; Drancourt, M. Beyond ancient microbial DNA: Nonnucleotidic biomolecules for paleomicrobiology. *BioTechniques* **2011**, *50*, 370–380. [CrossRef] [PubMed]

106. Minnikin, D.E.; Lee, O.Y.-C.; Wu, H.H.T.; Besra, G.S.; Donoghue, H.D. Molecular markers for ancient tuberculosis. In *Understanding tuberculosis—Deciphering the secret life of the bacilli*; Cardona, P.-J., Ed.; Intech: Rijeka, Croatia, 2012; pp. 3–36. ISBN 978-953-307-946-2.

107. Smith, N.H.; Hewinson, R.G.; Kremer, K.; Brosch, R.; Gordon, S.V. Myths and misconceptions: The origin and evolution of *Mycobacterium tuberculosis*. *Nat. Rev. Microbiol.* **2009**, *7*, 537–544. [CrossRef] [PubMed]

108. Brites, D.; Gagneux, S. Co-evolution of *Mycobacterium tuberculosis* and *Homo sapiens*. *Immunol. Rev.* **2015**, *264*, 6–24. [CrossRef] [PubMed]

109. Achtman, M. How old are bacterial pathogens? *Proc. R. Soc. B* **2016**, *283*, 20160990. [CrossRef] [PubMed]

110. Robbins, G.; Tripathy, V.M.; Misra, V.N.; Mohanty, R.K.; Shinde, V.S.; Gray, K.M.; Schug, M.D. Ancient skeletal evidence for leprosy in India (2000 B.C.). *PLoS ONE* **2009**, *4*, e5669. [CrossRef] [PubMed]